University of Lisbon

Faculty of Pharmacy

Mathematical Modelling for Development, Scale-up and Optimization of a Process of Lyophilisation

Mauro Luís Amado Duarte

Dissertation supervised by Prof. Dr. João F Pinto and co-supervised by Eng. João Moreira

Master Degree in Pharmaceutical Engineering

2018

Education is our passport to the future, for
tomorrow belongs only to the people who prepare for it today.
MALCOM X

Acknowledgments

I would like to start by showing my gratitude to Prof. Costas Pantelides and Dr. Sean Bermingham for the opportunity of doing the internship at Process Systems Enterprise.

I want to thank my supervisor, Prof. João Pinto, for letting me know about this opportunity, for encouraging me to accept this challenge and for all the help.

To my supervisor at PSE, João Moreira, I am really grateful for your guidance, ideas, dedication and friendship.

To my friends at PSE, Artur, Cristian, Francisco, Lilya, Mariana, Renato and Sugandha, thank you very much for the warm welcome and the unforgettable experiences that i shared with all of you. I hope to see you again, soon.

I would like to thank all my friends, specially Ana Rita, Andreia, António, Daniel, Inês, Miguel and Tiago for, despite the distance, making me feel like i have never left home.

To my roommates, Alexandre, Diogo and Patricia, thank you for being my second family, for all the laughter and support during this internship. Cheers mates!

Finally to my family, I would like to thank you for always being there for me, leading me in the right direction, specially my mother that always believed in me and supported all of my decisions.

Resumo

A liofilização é um processo importante na indústria farmacêutica, pois permite a conservação e estabilização de fármacos instáveis em meio líquido. O processo já é conhecido pela Humanidade desde os tempos pré-históricos, mas só na história recente se descobriu as vantagens deste processo, e atualmente é um dos processos mais usados na indústria farmacêutica, sendo que os produtos liofilizados (tanto farmacêuticos como alimentares) geram mais de 16 mil milhões de dólares por ano, valor este comparável à comercialização de equipamentos e serviços de liofilização. O processo já é tão usado, que em 2011, 41% dos novos medicamentos injetáveis eram liofilizados, sendo que em 1998 essa percentagem correspondia apenas a 11.9%.

O processo de liofilização é normalmente feito em batch e é realizado dentro de frascos que estão inseridos dentro de um liofilizador sendo este processo dividido em cinco passos, começando pelo passo de congelamento, passando a secagem primária, a secagem secundária, o empacotamento e o armazenamento do produto. Durante o passo de congelamento, o produto em estado líquido que se encontra dentro de frascos é congelado até atingir temperaturas a rondar os -40°C. Este passo é essencial de forma a determinar a estrutura cristalina do gelo, que irá determinar se o produto poderá ser seco de todo e em que condições é que a secagem terá de ser feita. O passo seguinte é a secagem primária, sendo o passo mais longo do processo e é quando ocorre a sublimação do gelo (transição diretamente do estado sólido para o estado gasoso). De modo a isso acontecer, a pressão dentro da câmara de liofilização é diminuída até valores abaixo dos 130 Pa e a temperatura da prateleira onde os frascos estão colocados é aumentada, de modo a aumentar a força motriz para o processo ocorrer, sendo este governado pela transferência de calor para a frente de sublimação e pelo transporte de vapor de água através do produto seco. Durante o processo é necessário garantir que a temperatura do produto não ultrapassa a temperatura de colapso do produto, pois acima dessa temperatura, o produto perde a sua integridade física, não podendo ser comercializado. Após isso ocorre a secagem secundária, onde se dá a desorpção da água que está adsorvida ao produto quando a temperatura da prateleira é aumentada de novo, desta vez para temperaturas entre os 25 e 50°C, durante várias horas de modo a quebrar as ligações entre a água e o produto. Depois da última secagem, o frasco onde se encontra o produto é tapado, sendo que este tem

de ser impermeável tanto a água como ao oxigénio. Após todos os frascos estarem tapados, estes são armazenados, e podem durar 100 ou até 1000 vezes mais tempo do que produtos fabricados usando processos convencionais de secagem.

Todo o processo de liofilização acontece dentro de liofilizadores, que estão disponíveis na escala laboratorial, piloto e industrial. O equipamento é constituído por várias partes, sendo elas o sistema de computador, o sistema de instrumentação, o sistema de vácuo, o sistema de refrigeração e a câmara do produto onde ocorre a liofilização.

A indústria gasta milhões de dólares por ano no desenvolvimento de processos industriais. De modo a reduzir tempo e custos no desenvolvimento, a indústria farmacêutica está a começar a usar modelos.

Neste trabalho resumem-se e comparam-se alguns dos modelos conhecidos na literatura para os três principais passos da liofilização, e os softwares disponíveis que usam os modelos referidos anteriormente. Há três tipo principais de modelos descritos na literatura, os modelo de uma dimensão em estado estacionário, os modelos dinâmicos de uma dimensão e os modelos dinâmicos de duas dimensões. O modelo de uma dimensão em estado estacionário só está disponível para a secagem primária, sendo este um modelo simples e capaz de prever as variáveis-chave da secagem primária, mas devido a essa simplicidade não é capaz de simular o comportamento dinâmico de um processo de liofilização, especialmente a variação de temperatura da prateleira. Modelos dinâmicos de uma dimensão estão disponíveis para a secagem primária e secundária e sendo modelos mais complexos, conseguem descrever o comportamento dinâmico do processo, mas este aumento na complexidade do modelo também aumenta a dificuldade em implementa-lo. No caso dos modelos dinâmicos de duas dimensões, estão descritos na literatura para o passo de congelamento, e para a secagem primária e secundária. Ao adicionar uma segunda dimensão ao modelo, permite descrever melhor as variações que ocorrem durante o processo, mas este tipo de modelos é de uma maior complexidade mais difíceis de implementar. Há poucos softwares disponíveis que usem as equações dos modelos referidos anteriormente, sendo que para o passo de congelamento, não existe nenhum software disponível. Usando o modelo de uma dimensão em estado estacionário, existem dois softwares disponíveis, o LyoModelling Calculator e o LyoCalculator, conseguindo prever variáveis como temperatura do produto e duração do processo para a secagem primária. A Process Systems Enterprise tem um modelo implementado em gPROMS usando a abordagem do modelo dinâmico de uma dimensão, que é capaz de prever e otimizar a secagem primária e a secagem secundária. Usando a abordagem mais complicada, os modelos dinâmicos de duas dimensões, existe disponível online o Passage/ FreezeDrying, que consegue prever variáveis-chave do processo de liofilização durante a secagem primária e secundária.

As equações do modelo de estado estacionário foram implementadas no gPROMS,

uma interface para o utilizador foi construída usando a linguagem XML e o modelo foi então validado recorrendo a uma calculadora online que também usa as equações do modelo em estado estacionário (*LyoModelling Calculator*) e posteriormente validado usando dados experimentais retirados de um artigo cientifico. Procedeu-se ao estudo do modelo implementado , onde em primeiro lugar uma analise de sensibilidade usando a ferramenta *Global System Analysis* (GSA) do gPROMS foi feita de modo a determinar quais dos parâmetros chave do processo tinham maior influência sobre os resultados e numa segunda parte do estudo, as capacidades preditivas e de otimização do modelo implementado foram comparadas com as de um modelo dinâmico de uma dimensão, previamente implementado em gPROMS.

Os resultados indicaram que quando o modelo foi validado usando o *LyoModelling Calculator*, foi possível obter os mesmos resultados que se obtiveram na calculadora, usando os mesmos parâmetros tanto no modelo como na calculadora, obtendo erros relativos inferiores a 2%. Na validação com os dados experimentais o modelo foi capaz de prever com exatidão os perfis de temperatura do produto ao longo de um processo real, com erros relativos inferiores a 3%.

Ao realizar a analise de sensibilidade, verificou-se que o coeficiente de transferência de calor do frasco tinha uma maior influência na temperatura máxima do produto, enquanto que a resistência a transferência de massa, tinha uma maior influência na duração do processo. Observou-se também que a pressão da câmara de liofilização tinha menor influência na temperatura máxima do produto e no tempo total de duração do processo, quando comparado ao coeficiente de transferência de calor do frasco e a resistência a transferência de massa.

A comparação com o modelo dinâmico de uma dimensão demonstrou que as capacidades preditivas de ambos os modelos são equiparáveis, mas em relação as capacidades de otimização, o modelo em estado estacionário não era o mais indicado para ser usado em otimização de processos.

Com este trabalho foi possível obter um modelo que pode ser usado na previsão da secagem primária, e conhecer tanto as vantagens como as limitações do mesmo.

Palavras-chave: Liofilização, Modelação, gPROMS

Abstract

Lyophilization is an important process in the pharmaceutical industry in order to stabilize drugs that are not stable in the liquid state. The industry spends millions of dollars per year in the development of industrial processes. The industry is turning to the use of models to reduce costs and time with the development of the process.

In this work, an overview of the existing models in the literature for the three mains steps of the lyophilization process is made and the main differences between the models are addressed and an overview of the software available that use said models is also made. The equations of the model for the primary drying step using the steady-state approach were implemented in gPROMS platform and the model was then validated against an online calculator that uses the same equations (LyoModelling Calculator) and against experimental data. Then, a study of the model implemented was carried out, first with a sensitivity analysis using the Global System Analysis (GSA) tool of gPROMS in order to determine which of the key parameters had the most influence on the output of the model, proceeding then to the second part of the study were the predictive and optimisation capabilities of the model were compared with a more complex model (one-dimensional dynamic model) already implemented on gPROMS.

The results showed that when the model was validated with the LyoModelling Calculator, it was able to give the same outputs. Regarding the validation with experimental data, the model was able to predict with accuracy the product temperature profile of a real process, with relative errors below 3%. The sensitivity analysis suggested that the vial heat transfer coefficient had the most influence in the maximum temperature of the product and the resistance to mass transfer had the most influence on the total duration of the process and the comparison with the one-dimensional dynamic demonstrated that the predictive capabilities of both models are similar, but the steady-state model implemented was not indicated to optimise a process.

With this work, it was possible to obtain a model that is able to predict the primary drying step and it allows to know the strengths and limitations of said model.

Keywords: Lyophilization, Modelling, gPROMS

Contents

List of Tables

List of Figures

List of Abbreviations

Acronyms

1D	One-dimensional
2D	Two-dimensional
FDA	Food and Drug Administration
gFP	gPROMS FormulatedProducts
GMP	Good Manufacturing Practice
GSA	Global System Analysis
MTM	Manometric Temperature Measurement
NIR	Near-infrared
PAT	Process analytical technology
PLC	Programmable Logic Controller
PSE	Process Systems Enterprise, Ltd
QbD	Quality by Design
RMF	Residual Moisture Final
SS	Steady-state
TDLAS	Tunable Diode Laser Spectroscopy
USS	Unsteady-state
WTO	World Trade Organization
WWII	Second World War

Greek Letters

α_{Ie}	Thermal diffusivity of dried region
α_{II}	Thermal diffusivity of frozen region
ΔH	Enthalpy of sublimation
ΔH_v	Enthalpy of vaporization
ε_p	Porosity of the product
ρ_{Ie}	Density of dried region
ρ_{II}	Density of frozen region
ρ_{sol}	Density of solution
ρ_w	Density of water

Symbols

A_1	Resistance constant
A_2	Second resistance constant
A_p	Product cross-sectional area
A_v	Vial cross-sectional area
c	Solid concentration
C_{Ie}	Specific heat capacity of the dried region
C_{pg}	Specific heat capacity of the gas
c_{pw}	Concentration of water vapour in the dried region
c_{sw}	Concentration of bound water
$D_{wIn,e}$	Effective diffusion coefficient
g	Equilibrium sorption isotherm
i	Number of the slice being dried
k_i	Effective thermal conductivity

k_v	Vial heat transfer coefficient
k_{Ie}	Thermal conductivity of the dried region
k_{II}	thermal conductivity of the frozen region
L	Length of the tray
l	Length dried
l_m	Initial length
m	Mass of ice
M_w	Molecular weight of water
n	Number of slices
N_t	Total molar flux
P_0	Vapour pressure of ice in the sublimation front
p_w°	Partial pressure of water at the surface
p_{wX}	Partial pressure of water at the sublimation front
q_I	Heat flux from the top
q_{III}	Heat flux from the side
q_{II}	Heat flux from the bottom
R	Ideal gas constant
R_0	Initial resistance to mass transfer
R_p	Resistance to mass transfer
S_i	First-order effect index
S_{Ti}	Total effect index
T°	Initial temperature
T_0	Sublimation front temperature
T_c	Collapse temperature
T_g'	Glass transition temperature

T_I	Temperature of dried region
T_I°	Temperature of the dried region at the surface
t_n	Drying time at ech slice
T_p	Temperature of the product at the bottom
T_s	Shelf temperature
T_{II}	Temperature of frozen region
t_{total}	Total drying time
V	Fill volume
V_p	Velocity of the gas in the dried region
V_s	Velocity of the sublimation front
N/A	Not applicable

Chapter 1

Introduction

Lyophilization, also known as freeze-drying, is a drying process widely used in the pharmaceutical and food industries to stabilize drugs and foods that are not stable in the liquid medium. The process is also used to improve and facilitate both the storage time and the transport of the products[1, 2, 3, 4]. In the pharmaceutical industry it is mostly used in the drying of heat-sensitive injectable drugs like vaccines, antibiotics and protein-base drugs that, being sensitive to high temperatures, may lose their stability and effectiveness when conventional drying processes are used. The powder that is formed at the end of the lyophilization process has a long shelf life and can be mixed with water and regain it's activity. The process occurs when a solution, usually aqueous, is frozen and the ice is removed by sublimation in a vacuum environment and it involves 5 steps. The first one is the freezing of the medium, the second is the primary drying in which the sublimation of the water occurs. The third step is the secondary drying where the desorption of the liquid that has not been sublimated in the previous step occurs. The fourth step is the packing of the dried product and the last step is the storage of the product, which may last 100 or 1000 times longer than products manufactured by conventional drying methods [1, 2, 3, 5]. Nowadays, spray-freeze-drying (a variation of the freeze-drying process, in which the spray-drying process is fused with the freeze-drying process) is being widely used for particle size engineering. In this process, the liquid product is atomised (liquid is divided into a large number of small droplets), then the droplets formed are frozen and then the sublimation of the ice occurs, resulting in particles with a determined size [6] .

Lyophilized pharmaceuticals has taken on greater prominence in the parental industry, making half of new injectable or infusible drugs introductions by 2015, but it still remains as one of the most time-consuming and expensive unit operations in the pharmaceutical industry [2, 7].Thus, in order to reduce costs and time of operation, and improve quality, a better optimisation of the process in necessary which can be achieved through the modulation of the process.

1.1 Background

Lyophilization is a process known to mankind since pre-historical times. Since 1250 BC, ancient Peruvian Incas placed potatoes at the top of Machu Picchu, causing the food to freeze, and the low pressure at high altitude sublimated the water from the potatoes, hence freeze-drying. Ancient Eskimos are also known to have placed fish in the cold of the Arctic, freezing and drying it [5, 8, 9].

Only in recent History that we realized the advantages of the lyophilization process. In 1890, Richard Altmann reported that he was able to dry a human tissue, using sub atmospheric pressures and temperatures of -20°C [8]. In 1933, Earl Flosdorf and Stuart Mudd successfully preserved human serum through freeze-drying and during the World War II the process was developed commercially in order to preserve blood plasma and penicillin, saving countless lives during the war [10].

The best-known product produced by lyophilization, freeze-dried coffee, was first manufactured in 1938 when Brazil asked Nestlé to develop a method to store and preserve their supply of coffee [8, 10].

After this, lyophilization become one of the most important processes for the preservation of heat-sensitive pharmaceuticals, and FDA in 1963 set the first Good Manufacturing Practice (GMP) for the freeze-drying of pharmaceuticals products and in 1969, the World Trade Organization (WTO) approved a resolution to execute the GMP of freeze-dried pharmaceuticals [10].

The process is widely used in both pharmaceutical and food industries and in 2015, 5 of the 10 top-selling drugs were lyophilized [2, 8, 10].

Nowadays, the lyophilization of mammalian cells (specially sperm and stem cells) is possible using lyoprotectants (products used to protect cells from the drying process) such as sugars, poly-alcohols and their derivatives. With this, is possible to have a method to replace the cryo-preservation of stem cells with lyophilization, allowing for a easier and cheapest way to storage, transfer and prevent the contamination of the sample [11, 12, 13, 14].

Lyophilization is a process vastly described in the literature [5, 8, 9, 10, 15]. Models describing the primary drying and secondary drying of the lyophilization process are also available in the literature, being the more important models described by Pikal and Liapis [16, 17, 18, 19]. Models describing the freezing step are also described, but not in the same extent as the previous ones [20].

1.2 Lyophilization market

Lyophilization is widely used in pharmaceutical industry and the food industries and according to the LyoHub group, the worldwide market for lyophilized food and

pharmaceuticals is approximately 16 thousand million dollars per year, a value that is matched by the market for lyophilization equipment and services. Although lyophilized food counts for the largest slice of the lyophilized products, the lyophilized biologics (includes recombinant protein drugs, vaccines, and blood products) have the greatest growth rate per year [21].

Since the beginning of the millennium, the number of lyophilized drugs inserted in the market per year increased significantly. The oncology, infectious and metabolic diseases lyophilized drugs make the most part of the newly approved lyophilized drugs per year, as can be seen in Figure 1.1.

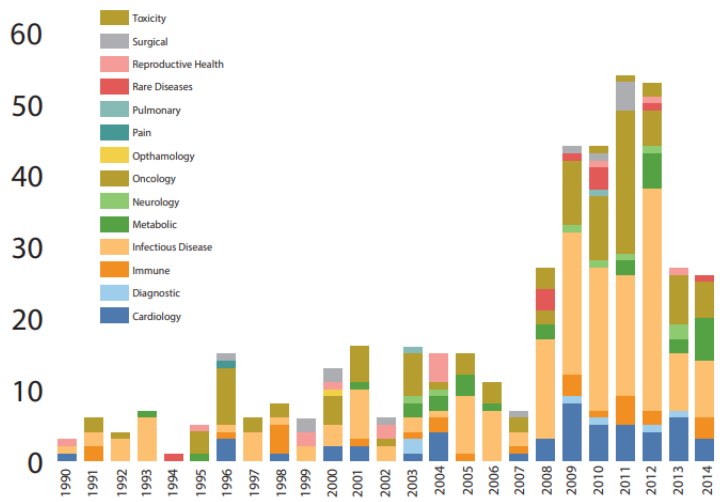

Figure 1.1: Number of newly approved Lyophilized drugs per year[21].

From 1990 to 1998, newly approved lyophilized drugs made about 11.9% of all injectable/infusible drugs. In 2011 it was 41% and in 2013-2015 it was half of the approvals, demonstrating the growth in the lyophilized drugs[21].

1.3 Lyophilization process

1.3.1 Process description

The lyophilization is usually a batch process that is performed in vials placed in shelves inside a freeze-dryer and it is divided in five main steps [22, 23].

Freezing step

The first step is the freezing of the liquid medium (usually water) containing the active substance at atmospheric pressure. Usually, for the freezing step, the temperature of

the shelf is decreased, in several stages, to a temperature around -40°C, solidifying most of the water into ice [10, 22, 23].

This step is really important because it dictates the structure of the frozen product and it is highly dependent of the amount of nuclei available for crystallization, the freezing rate and the end temperature of the freezing step. The structure of the frozen product dictates if the product can be dried at all, the maximum temperature at which the ice can be sublimed to avoid collapse of the cake, the pressure at which the remaining water must be desorbed, the minimum water content that can be achieved at the end of the lyophilization, and at which temperature, and for how long the product can be stored. At slow freezing rates ($<$ 0.5°C/min), water crystallizes to a maximum extent, forming larger ice crystals than at quick freezing rates (0.5-2°C/min). Rapid freezing rates (5-100°C/min) can only be achieved using liquid nitrogen and mostly small ice crystals are formed. Most drugs (e.g proteins) are solidified in an amorphous glass, containing large amounts of unfrozen water adsorbed [22, 23].

In order to get better crystal size uniformity, annealing can be used. Annealing is a processing step in lyophilization in which samples are kept at a given sub-freezing temperature above the glass-transition temperature (T_g'), for a certain amount of time, before decreasing the temperature back to the freezing temperature. The annealing allows bigger ice crystal to grow, instead of the small ones, resulting in a more porous product, leading to a reduced resistance to mass transfer in the product. This reduced resistance can make the primary drying process faster. [24, 25, 26, 27].

Primary drying

The second step is the primary drying which is based on the sublimation phenomenon, which is the transition of a substance directly from the solid state to the gas phase without passing through the liquid phase. The process is illustrated in the phase diagram of pure water in Figure 1.2.

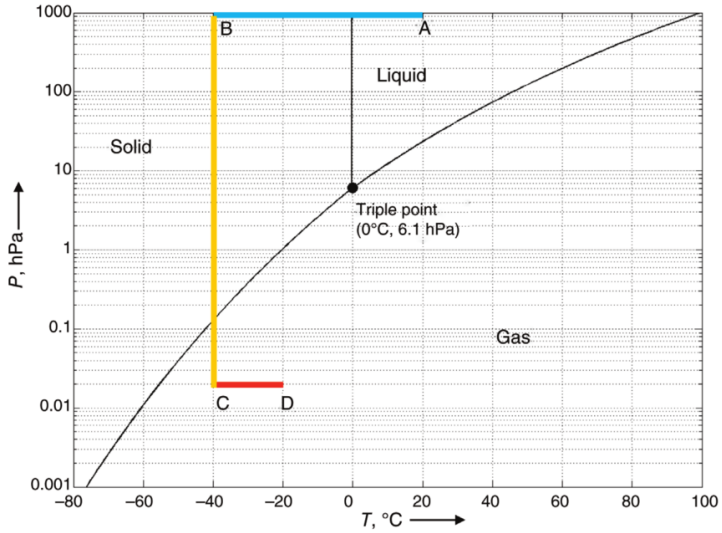

Figure 1.2: Phase diagram of pure water[15].

In this step, after the freezing step (A to B in Figure 1.2) , the pressure inside the chamber is reduced using a vacuum pump (B to C in Figure 1.2), usually to values below 130Pa (1.3×10^{-3}atm) and then the shelf temperature is increased (C to D in Figure 1.2),increasing the driving force for the sublimation of ice. This process forms a dried cake, and the vapour escapes the cake through the porous dried layer[10, 22].

In this step, the sublimation of ice is mostly governed by heat transfer to the sublimation front and transport of water from the ice front through the dried product. This two phenomena, that occurs at the same time, are the ones who influence the primary drying time the most. At the end of this step, there is still approximately 10% of water adsorbed to the dried cake [10, 22].

In the primary drying, it is critical to not let the temperature of the product exceed the collapse temperature (T_c). During the primary drying, above this value, it is possible to observe a loss in structure in the dried region adjacent to the sublimation front due to a glass transition in the amorphous product. The collapse will be the cause to rejection of the product simply because it lacks "elegance". it is also necessary to take in account the glass transition temperature (T_g'), that is the temperature at which the glass transition occurs in the amorphous phase in contact with the ice, and is usually 2°C below the collapse temperature. A microscopic collapse usually occurs above the glass transition temperature, but only in rare occasions a macroscopic collapse occurs.So, the collapse temperature is assumed to be the maximum allowable product temperature for primary drying [28, 29].

Secondary drying

The third step is the desorption of the remaining water adsorbed to the dried cake, or secondary drying. In this step, the temperature is further increased to temperatures

around 25-50°C for several hours in order to break any interaction formed between the adsorbed water and the material, transforming the adsorbed water in free water and evaporating it. At the end of the secondary drying, there is still a residual moisture final (RMF) that cannot be neither too high or too low (between 0.3 and 3%). With a RMF too low, the product lose part of it's activity and with a too high RMF, it is not suitable for long-term storage. [10, 22, 23, 30]

Packing

After the primary and secondary drying, there is a fourth step of packing. The packaging needs to be both oxygen and water-tight. To achieve this, the vials are placed with a stopper in a semi-open position inside the shelves and at the end of the process, the stopper is pushed to the closed position under vacuum [22].

Storage

After all the vials are closed, the product is stored under certain conditions possibly lasting 100 or even 1000 times longer than the products manufactured by conventional drying processes [22].

1.3.2 Freeze dryer

The freeze dryer, or lyophilizer, is the equipment where the lyophilization process takes place, existing in laboratory, pilot and industrial scales. The design of the equipment can strongly influence the quality of the product, so the choice of the freeze dryer is crucial. The freeze dryer is comprised of various components that usually include the computer, instrumentation, vacuum, refrigeration systems and the product chamber[31, 32, 33, 34].

Computer System: The Computer System: computer system is normally a programmable logic controller (PLC), and it usually has a temperature and pressure sensing ability. it is one of the most overlooked aspects of freeze-drying but is important to keep the system running at peak efficiency [31, 32].

Instrumentation System: The instrumentation system includes all of the temperature and pressure sensors inside the lyophilizer and is usual to have at least 2 or 3 types of instrumentation system that requires calibration [31, 32].

Vacuum System: The vacuum system contains a vacuum pump and a ice condensing chamber.The vacuum pump can be either a direct drive pump with oil lubrication or an oil-free vacuum pump. The oil lubricated vacuum pump can reach very low pressures

(below 10mTorr) and are relatively cheap, being the most used vacuum pumps in the industry. This type of vacuum pumps need to have the oil exchanged in periods of 2000-3000 hours of use. The oil-free vacuum pumps don't need the oil changes, they do require a periodic rebuilding because of lack of lubrication. This type of vacuum pumps are not as used in the industry, because they don't achieve pressure as low as the oil lubricated ones. The ice condensing chamber condense the water vapour turning it into ice again, to avoid the chamber pressure to increase as a result of the water vapour inside. At reduced pressures, even small amounts of ice (for example, 1g) produces large amounts of water vapour (100 m^3), therefore the ice condenser removes large volumes of vapour inside the chamber. The condenser can be located inside the drying chamber (internal condenser) or in a separate chamber connected to the product chamber (external condenser) [15, 31, 32]. A example of a oil-lubricated vacuum pump is shown in Figure 1.3.

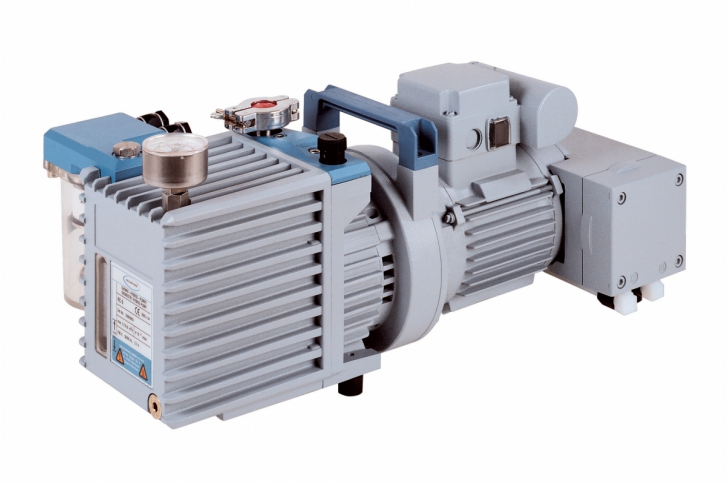

Figure 1.3: Oil-lubricated vacuum pump[35].

Refrigeration System: The refrigeration system is used to cool the condenser, in order to be possible to condense the water vapour and it can also be used to cool the shelves, in order to freeze the product [15, 31, 32] .

Product Chamber: The product chamber is a large space with a system of shelves on which the product, either a tray or vials are placed. The shelves are heated and provide the heat for the sublimation to occur. [15, 31, 32].

The freeze-dryers can be divided into three categories, laboratory freeze dryers, pilot freeze dryers and industrial freeze-dryers, according to the scale they are used in.

Laboratory freeze dryer

The laboratory freeze-dryers are the smallest and are normally used to remove water content of a product in clinical trials and to draft a protocol development for scale-up. These kind of equipment, can be classified in manifold dryers and shelf dryers[31, 36, 33]. The manifold dryers are often used as the entry equipment to lyophilization, being used mostly in the initial steps of investigation and a typical manifold dryer can be seen in Figure 1.4 [31, 36].

Figure 1.4: Typical manifold freeze dryer[31].

With a manifold dryer, flasks are filled with the product proceeding to the freezing step that occurs away from the equipment, thus it cannot be well controlled. After, the flasks with the frozen product are introduced to the equipment via a vacuum valve, the pressure is reduced using the vacuum, initiating the primary drying. The heat for the sublimation is provided by the surrounding environment, making it hard to control the process. In the secondary drying, the water adsorbed into the product is removed using the vacuum pump. With these equipment the process is hard to control, therefore it is only used in the initial stages of investigation[36].

The shelf dryers have shelves inside the product chamber, where vials or trays with the product are placed. In these kind of equipments, it is possible to do the freezing, primary and secondary drying steps, by controlling the temperature of the shelves . The laboratory freeze-dryers can handle from 2 to a few hundred vials [31, 32, 33] .

Pilot freeze dryer

The pilot freeze-dryers are mainly used to small scale production and to do scale-up to the industrial scale and only shelf dryers are available. These equipments can be filled with a few thousand vials [33].

Industrial freeze dryer

Industrials freeze dryers are used for big scale production and only shelf dryers are available. The biggest freeze dryers have a maximum capacity to over 500 thousand vials at the same time, and a example of a industrial freeze dryer can be seen in Figure 1.5

Figure 1.5: Industrial freeze dryer[37].

1.3.3 Control of the process

The United States Food and Drug Administration (FDA) in 2004 released a document encouraging the use of process analytical technology (PAT), in order to enhance understanding and control of the manufacturing process. PAT is a system for designing, analysing, and controlling manufacturing through timely measurements of critical quality and performance attributes. To accomplish that purpose, several in-line tools to monitor and control the temperature were developed, such as Near-infrared (NIR) and Raman spectroscopy. Other methods of controlling the process such as the the placement of thermocouples, manometric temperature measurement (MTM) and tunable diode laser

absorption spectroscopy (TDLAS) are also used, mostly to control the temperature of the product[38, 39, 40, 41].

Thermocouple measurement: Thermocouples can be inserted inside some of the vials, properly selected, in order to measure the temperature of the product. Usually, thin wired thermocouples are used in the laboratory scale freeze dryers and wireless ones are often used in the industrial scale freeze dryers. The thermocouples can only be used to measure the product temperature at one location at a time (usually the bottom) and the readings from the last third of the process cannot be trusted because the heat from the thermocouple is transferred to the product, resulting in a hole in the frozen product, making a connection between the thermocouple and the chamber. When this happens, the thermocouple begin to measure the temperature of the chamber instead of the temperature of the product, resulting in a sharp increase in the temperature measured. Moreover, when the thermocouple is introduced, it acts as a heterogeneous nucleation site, resulting in bigger crystals formed, and a lower resistance to mass transfer, that makes the vials probed with the thermocouples have shorter lyophilization cycles than the ones without the thermocouple [41, 42, 43, 44, 45].

Manometric temperature measurement (MTM): The MTM is a method in which the temperature of sublimation front during the primary drying can be measured without putting any device inside the vial. In this method, the valve connecting the chamber to the condenser is quickly closed and the variation of pressure with time in the chamber is measured. An algorithm analyses the data and calculate the pressure at the sublimation front and the product resistance to the mass transfer. Based on these calculated variables, another algorithm calculates the heat transfer, the temperature of the sublimation front and the vial heat transfer coefficient [45, 46, 47, 48].

Despite the multiple uses of MTM, the temperature that is measured is the average of all the vials inside the chamber and this average is heavily weighted in favour of the lower temperature vials [46, 47].

NIR spectroscopy: NIR spectroscopy is a fast, non-destructive and non-invasive technique that provides multi-variable analysis for virtually any product. The wavelength extends from the mid-infrared to the visible light (from 780 to 2526nm). In the recent years it has gained great importance in the pharmaceutical industry, specially for raw materials testing, product quality control and process monitoring. This vibrational spectroscopic technique doesn't require a sample preparation beforehand , and physical and chemical properties can be predicted in a single spectrum. However, water has such a strong signal in the NIR spectra (being really useful to monitor the moisture of the product) that in this process overwhelms the signals from other compounds in the formulation. To counter this, a combination of NIR and Raman spectroscopy is used [39, 40, 49].

Raman spectroscopy: Raman spectroscopy, such as NIR, is a vibrational spectroscopy that is fast, non-destructive and non-invasive. In Raman spectroscopy, a laser is focused into a sample, and the inelastic scattered radiation (Raman scattering) is optically collected and directed into a spectrometer that detects the photon energy and separates by wavelength. Compounds such as drugs can be detected and identified by their specific frequency and quantified by the intensity of the peaks. In Raman spectroscopy, contrary to NIR, the spectra contain sharp bands by which the compounds can be identified. However, water has a weak peak in a Raman spectrum, making it hard to monitor the moisture content. Raman and NIR spectroscopy can be considered as useful complementary tools for monitoring freeze-drying processes [39, 50].

Tunable diode laser absorption spectroscopy (TDLAS): TDLAS is a unit that is installed in the duct connecting the chamber to the condenser, that has two laser beams that emits NIR radiation, one of them directed in the same direction of the flow of the vapour and the other direct against said flow, with a detector on the opposite side of each laser, as it is outlined in Fig.1.6. This system allows for a continuous and in real-time measure of the concentration of selected gases. TDLAS is used nowadays to measure the sublimation rate of the lyophilization process both in laboratory scale and industrial scale. [51, 52, 53].

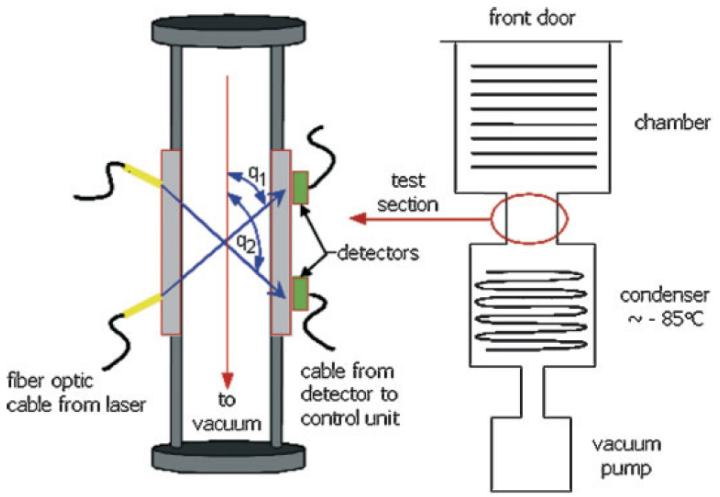

Figure 1.6: Schematic of the tunable diode laser absorption spectroscopy (TDLAS) equipment [52].

1.4 Motivation

The lyophilization process is widely used in the pharmaceutical industry but despite that, it is one of most time-consuming and expensive unit operations, having undergone

few changes since it was introduced in 1940. This can be attributed to the fact that it is a very complex process that involves complex heat and mass transfer phenomena, requiring knowledge of engineering, chemistry and biology to understand [2, 54]. The lack of real-time monitoring to determine attributes such as the product temperature, due to constraints imposed by the aseptic processing requirements for injectable drugs is driving the industry to alternatives, like modelling of the process [7]. In the past the development of the process, in both laboratory and industrial scales, was through trial and error leading to high costs in development. Nowadays, the industry is turning to the use of models to minimise this cost, focusing on the optimisation of the primary drying step, which is the longest and most complicated step. The table 1.1 shows the results of a survey done to 11 companies in 2015, in order to understand how modelling was used in the freeze-drying operations in each company. 5 companies out of the 11 surveyed used modelling in lyophilization processes [54].

Table 1.1: Results of a survey where five companies (listed by numbers) out of 11 surveyed, were using modelling in freeze-drying operations[54].

Applications of Primary Drying Model	**Company**				
	#1	#2	#3	#4	#5
Process Development	x	x	x	x	x
Scale-up and transfer	x	x	x	x	x
Deviation analysis and decision making			x		x
Process optimization	x	x	x	x	x
Provides suitable feedback to regulatory authorities					x

Out of the 5 who used modelling, all of them use models for process development, scale-up and transfer and for optimization, two of them use for deviation analysis and decision making and just one of the companies use modelling to provide feedback to regulatory authorities[54].

On top of that, the pharmaceutical industry is starting to use Quality by Design (QbD) approaches in order to demonstrate to the regulatory agencies the understanding and capability of the processes. In order to do that, defining a design space is crucial. In order to study the design space in a lyophilization process, numerous experiments runs would be necessary to be done, increasing substantially the costs for the development of the process. Using models to define the design space, the costs associated with the investigation of the design space can be reduced, allowing for savings in the order of millions of dollars [55, 56].

In this regard, better models are necessary to counter the "it's always been done that way" dogma and helping in the continuous improvement of lyophilization and to create more profitable processes [2].

1.5 Scope

The current work aims to bring a better understanding of the different types of model available in the literature for the lyophilization process.It is intended to discuss the implementation in the gPROMS platform and validation of a model for the primary drying step and test the limitations and applicability of these model in the development, scale-up and optimisation of the process. The comparison between the model to be implemented and an existing model of the gPROMS platform will also be addressed in the current work.

With the implementation of the model, it is intended to obtain a model that can be used to predict the primary drying step and, using the gPROMS capabilities, to be able to optimise a process, in order to be used in an industrial process, something that most models available online cannot do.

1.6 Outline

In Chapter 2, an overview of the existing mathematical models in literature for the lyophilization process is going to be made.

In Chapter 3, a revision of the software platform in which the modelling of the current work is based on is presented, as well as the tools and capabilities of said software.

In Chapter 4, the implementation of a steady-state model for the primary drying is presented and the model is validated against an existing model and experimental data. A sensitivity analysis on the key parameters of the model is also presented, where the influence of the key parameters in the output is studied.

In Chapter 5, a case study is demonstrated where the predictive and optimisation capabilities of two different models for the primary drying step are compared with each other.

Finally, in Chapter 6, the main conclusions obtained are summarized and possible future work is discussed.

Within these chapters, it is intended to enlighten about the models described in the literature and the gPROMS platform, as well as the implementation, validation and study of a model for the primary drying step that was described in the literature.

Chapter 2

Models

2.1 Models

Over the years, many scientists developed models in order to predict the behaviour of the lyophilization process. Those models can be divided in three major categories: one-dimensional steady-state , one-dimensional dynamic and two-dimensional dynamic.

2.1.1 One-dimensional Steady state models

One-dimensional (1D) steady-state (SS) models were studied for many years but in literature, these type of models only exist for the primary drying step.

In 1967, Orville C. Sandall developed a steady-state model in which he relates the fundamental transport properties of the dried material to the observed drying rates. In his model, the equations representing the rates of heat and mass transfer to and from the frozen layer were addressed [57].

In 1984, Pikal evaluated mass and heat transfer resistances inside the vial and chamber-to-condenser mass and heat resistances. He described the primary drying phase, using equations to demonstrate mass transfer resistance from the vial to the chamber and to the condenser, and heat transfer resistance from the shelves to the vial. Regarding the mass transfer problems, he admitted that the water vapour is impeded by three barriers or resistances: resistance of the dried-product layer above the frozen product (which depend on the product itself and on the vial used), resistance of the semi-stoppered vial and the resistance in transfer from the drying chamber to the condenser. Regarding the heat transfer problem, he admitted that the heat is transferred to the product from the surface of the shelf in which the vial containing the product is placed, and the vial is placed directly on the shelf. The equations used for the resistance of the dried product and several aspects of heat transfer were already been addressed before [16, 58].

In the model of Pikal, the frozen product is divided into a n number of slices and within each slice, the parameters are considered to be constant. This model is simple, but it can determine accurately key variables of the process, such as product temperature and the duration of the primary drying, and it is still used in the industry nowadays in the development of the process [54, 16]

The equation describing the mass transfer of water vapour across the product (sublimation rate) is given by[16, 59, 60, 61]:

$$\frac{dm}{dt} = \frac{A_p(P_0 - P_c)}{R} \tag{2.1}$$

Where, A_p is the product cross-sectional area, P_0 is the vapour pressure of ice in the sublimation front, P_c is the chamber pressure and R_p is the resistance of the product to mass transfer at each slice. The resistance can be obtained using the following equation:

$$R_p = R_0 + \frac{A_1 l}{1 + A_2 l} \tag{2.2}$$

Where R_0 is the initial resistance, A_1 and A_2 are constants obtained experimentally and l is the length dried at a certain slice. In order to calculate the resistance to mass transfer, it is necessary to calculate the l, and the equation to obtain it is:

$$l = \frac{i l_m}{n} \tag{2.3}$$

Where n is the number of slices, i the number of the slice being dried and l_m is the initial solution length and can be given by:

$$l_m = \frac{V \rho_{sol}}{A_p} \left(\frac{1-c}{\rho_i} + \frac{c}{\rho_w} \right) \tag{2.4}$$

Where V is the fill volume of the vial, c is the solid concentration, ,ρ_{sol} is the density of the solution, ρ_i is the density of ice and ρ_w is the density of water. Usually the mass transfer resistance from the semi-stoppered vial and from the drying chamber to the condenser are neglected and only the mass transfer resistance of the product is taken in account.

The vapour pressure of ice is found as:

$$P_o = 2.6983 * 10^{10} e^{\frac{6144.96}{T_0}} \tag{2.5}$$

Where T_0 is the sublimation temperature at each time step.

The heat transfer is given by three equations, that include one that correlates the sublimation rate to the heat transfer. In this model, the heat is assumed to come in

only one direction, from the shelf where the vial is placed to the bottom of the vial. The equation that describe the heat transfer from the shelf to the vial is gives as:

$$\frac{dQ}{dt} = A_v k_v (T_s - T_p) \tag{2.6}$$

Where A_v is the vial cross-sectional area, the k_v is the Vial heat transfer coefficient, the T_s is the shelf temperature, the T_p is the temperature at the bottom of the product.

After this, the heat is transferred through the frozen product until the sublimation front (interface between the frozen product and dried product) and is given by:

$$\frac{dQ}{dt} = A_v k_i \frac{T_p - T_0}{l_m - l} \tag{2.7}$$

Where the k_i is the effective thermal conductivity of the product. The last heat transfer equation correlates the heat transfer with the mass transfer using the enthalpy of sublimation of ice (ΔH_s)

$$\frac{dQ}{dt} = \Delta H_s \frac{dm}{dt} \tag{2.8}$$

Using these three equations is possible to determine the temperature of the product, the temperature of the sublimation front and the amount of heat transferred in each slice.

In order to know the drying time of each slice (t_n) the following equation is used:

$$t_n = \frac{dm}{\frac{dm}{dt}} \tag{2.9}$$

Where the dm is the amount of ice in the vial and can be calculated in two different ways, depending if the product is crystalline or if it is amorphous. If the product is crystalline, the amount of ice is given by:

$$dm = V \rho_{sol} (1 - c) \tag{2.10}$$

And if the product is amorphous, it contains about 20% of unfrozen water, meaning that for every 4 parts of the product, there is 1 part of water. Thus the fraction of solute is multiplied by 1.25 to account for the water bounded to the structure [62]y:

$$dm = V \rho_{sol} (1 - 1.25c) \tag{2.11}$$

The total drying time (t_{total}) is the sum of all drying times at each interval and can be written as:

$$t_{total} = \sum_{n=i}^{n} t_n \tag{2.12}$$

With this equations, it is possible to describe a simple model, that can accurately predict key variables of the process. But because of the simplicity of the model, it is not possible to describe the dynamic behaviour of the process, specially the behaviour of the shelf temperature, from the beginning of the process until the end.

2.1.2 One-dimensional Dynamic models

The dynamic models (or unsteady-state) vary from the steady-state ones in the sense that the variables describing the process vary with time, instead of with the length of the product. This allows the model to capture more details of the process, but it makes the model more complicated. There are 1D dynamic models describing the primary drying and secondary drying steps. In 1979, Liapis and Litchfield made a two part work, where a mathematical model were developed using partial differential equations for the sublimation of ice in a single tray, assuming that heat and mass transfer occur in only one dimension and the sides and bottom of the tray are perfectly insulated against mass and heat transfer [17, 18].

In 1994,Liapis and Bruttini develop a new model where the dynamic behaviour of primary and secondary drying steps were described for amorphous and crystalline solutes [63, 64].

Primary drying step

Basing on the work of Liapis and Bruttini, the system describing the primary drying step are described below [63].

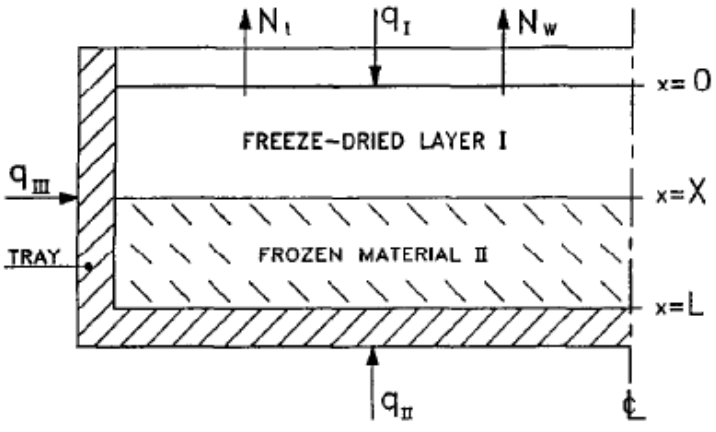

Figure 2.1: Schematic of a product in a tray during primary drying (variable X denotes the position of the sublimation interface front between the freeze-dried layer and the frozen layer)[63].

In Figure 2.1, a schematic of the system that the model describe is shown. In this system, a tray is placed inside a shelf, which provide heat from below (q_{II}). The heat

flux from the shelf above the tray (q_I) is also considered. The tray has a length L, which has a dried layer (I) and a frozen layer (II), being the boundary between both layers the sublimation front (X). The sublimation will occur as a result of the heat from the shelves being conducted to the sublimation front. The water vapour flows through the dried layer to the surface. There is heat from the side (q_{III}) but the magnitude is negligible when compared with the q_I and q_{II}. The equations used to describe the system are showed below [17, 18, 63].

The equation that demonstrate the temperature variation with time in the dried layer is given by:

$$\frac{\partial T_I}{\partial t} = -N_t \left(\frac{C_{pg}}{\rho_{Ie} C_{pIe}} \right) \frac{\partial T_I}{\partial x} + \alpha_{Ie} \frac{\partial^2 T_I}{\partial x^2} + \frac{\Delta H_v}{\rho_{Ie} C_{pIe}} \left(\frac{\partial c_{sw}}{\partial t} \right), \qquad 0 \leq x \leq X \tag{2.13}$$

Where, T_I is the temperature of the dried region, t is the time passed, N_t is the total molar flux, C_{pg} is the specific heat capacity of the gas, ρ_{Ie} is the density of the dried region, C_{pIe} is the specific heat capacity of the dried region, X is the distance from the sublimation front to the surface of the sample, α_{Ie} is the thermal diffusivity of the dried region, ΔH_v is the heat of vaporization of the water bound to the product and c_{sw} is the concentration of water bound to the product [17].

The equation for the variation of temperature in the frozen region is given by:

$$\frac{\partial T_{II}}{\partial t} = \alpha_{II} \frac{\partial^2 T_{II}}{\partial x^2}, \qquad X \leq x \leq L \tag{2.14}$$

Where T_{II} is the temperature of the frozen region, α_{II} is the thermal diffusivity of the frozen region and L is the length of the tray. The equations 2.13 and 2.14 show how the temperature of the dried region and frozen region, respectively, vary with time and space. At the beginning of the process, the temperatures of the frozen region and the dried region are equal to the initial sample temperature (T°), and it can be written like:

$$T_I = T_{II} = T^\circ, \qquad t = 0,\ 0 \leq x \leq L \tag{2.15}$$

The boundary conditions for the heat transfer are specified as:

$$q_I = -k_{Ie} \frac{\partial T_I}{\partial x}, \qquad x = 0,\ t > 0 \tag{2.16}$$

$$q_{II} = -k_{II} \frac{\partial T_{II}}{\partial x}, \qquad x = L,\ t > 0 \tag{2.17}$$

$$T_I = T_X = T_{II}, \qquad x = X,\ t > 0 \tag{2.18}$$

$$k_{II}\frac{\partial T_{II}}{\partial x} - k_{Ie}\frac{\partial T_I}{\partial x} + V_s(\rho_{II}C_{PII}T_{II} - \rho_I C_{PI}T_I) + N_t C_{Pg}T_I = \Delta H N_t, \qquad x = X \tag{2.19}$$

In equation 2.16, k_{Ie} is the thermal conductivity of the dried region. This equation indicates the heat flux at the surface of the tray. In equation 2.18, T_X is the temperature at the sublimation front and it gives the temperature at the sublimation front. In equation 2.19 K_{II} is the thermal conductivity of the frozen region, V_s is the velocity of the sublimation front, ρ_{II} is the density of the frozen region, C_{PII} is the specific heat capacity of the frozen region and ΔH is the enthalpy of sublimation.

The mass transfer equation for the water vapour is shown below.

$$\varepsilon_p\frac{\partial C_{pw}}{\partial t} + \frac{\partial}{\partial x}(V_p C_{pw}) + \frac{\partial C_{sw}}{\partial t} = \varepsilon_p\frac{\partial}{\partial x}\left(D_{win,e}\frac{\partial c_{pw}}{\partial x}\right) \tag{2.20}$$

Where ε_p is void fraction of the product (porosity), C_{pw} is the concentration of water vapour in the dried layer , V_p is the velocity of the gas in the porous dried layer,and $D_{win,e}$ is the effective diffusion coefficient of the vapour. The c_{sw} is given as :

$$\frac{\partial C_{sw}}{\partial t} = \left(\frac{\partial g}{\partial C_{pw}}\right)\left(\frac{\partial C_{pw}}{\partial t}\right) \tag{2.21}$$

Where g is the equilibrium sorption isotherm. At the beginning of the process, the concentration of vapour water is assumed to be 0 and the concentration of bound water is assumed to be equal in all the length of the product. The boundary equations for the mass transfer in the surface of the product and at the sublimation front are given by the equations (2.22) and (2.23), respectively.

$$C_{pw} = M_w\left(\frac{p_w^0}{RT_I^0}\right), \qquad x = 0, \quad t \geq 0 \tag{2.22}$$

$$C_{pw} = M_w\left(\frac{p_{wX}}{RT_X}\right), \qquad x = X, \quad 0 < t \leq t_{X=L} \tag{2.23}$$

Where in equation (2.22), the M_w is the molecular weight of water, p_w^0 is the partial pressure of water vapour at the surface, R is the ideal gas constant and T_I^0 is the

temperature of the dried region at the surface. Regarding the equation (2.23), p_{wX} is the partial pressure of water in the sublimation front.

The equation of the moving boundary of the sublimation front is given by:

$$V = \frac{dX}{dt} = -\frac{N_t}{\rho_{II} - \rho_{Ie}} \tag{2.24}$$

Secondary drying step

In the secondary drying step, there is no frozen layer, so there is not a moving sublimation interface. The equations describing the temperature of the dried layer is the same as the equation (2.13), but instead of being defined between 0 and the sublimation front, is defined between 0 and the length of the dried product (L). The initial temperature of the dried layer is equal to the final temperature of the dried layer in the primary drying model and the boundary conditions for the heat flux from above and below can be defined using the equations (2.16) and (2.17), respectively. The mass transfer equations can be defined using the equations (2.20) and (2.21).The initial concentration of the bound water and the vapour water, are the same at the ones at the end of the primary drying model [63].

With the 1D dynamic models, it is possible to describe the dynamic behaviour of both the primary and secondary drying, accurately predicting key variables of the process. But with this capability, the complexity of the model increases as well as the difficulty when implementing these type of models.

2.1.3 Two-dimensional Dynamic models

These type of models, assume two physical dimensions, counting both for the length and the width of the product.The main difference between these models and the 1D dynamic models, is that it accounts for the heat from the sides, making the heat and mass transfer in the width of the product not constant, as it was in the other models. Using two dimensions allows to better describe what happens during the freeze-drying process, because it does not ignore the influence of the heat from the side. 2D models were firstly studied by Mascarenhas and Pikal in 1997, where he described the primary step in a single vial [65].

In 1998, Liapis and Sheehan described both primary and secondary drying steps of two-dimensional approach [66].

In 2007, Nakagawa proposed a semi-empirical model for the freezing step of the freezing step, where using the two-dimensional approach, the mean crystal size can

be estimated, and consequently the permeability to the water flow (resistance to mass transfer) of a certain product [20].

2.1.4 Available Software

There are few software available that can be used to predict the properties of the lyophilization process, in the different main steps. For the freezing step of the process, there is no software available for this step.

There are two software on-line, the LyoModelling Calculator from SPScientific and the LyoCalculator from PharmaHub, that uses the 1D steady state approach.

Process Systems Enterprise (PSE), has a model using the 1D dynamic approach for the primary and secondary steps implemented in his software, gPROMS®.

Lastly, Passage® also has a model for the primary and secondary steps, but using the 2D dynamic approach instead. The summary of all the software available is shown in the Table 2.1

Table 2.1: Summary of software available for the modelling of the lyophilization process

Step	**1D steady-state model**	**1D dynamic model**	**2D dynamic model**
Freezing step	X	X	X
Primary Drying	LyoModelling Calculator LyoCalculator	gPROMS	Passage/FreezeDrying
Secondary Drying	X	gPROMS	Passage/FreezeDrying

Chapter 3

1D Steady state Model

In this chapter, the 1D steady-state model developed in gPROMS FormulatedProducts® will be addressed. The model was validated using the LyoModelling calculator and experimental data. A sensitivity analysis was also performed in order to better understand the model, and the influence the parameters have on the output.

3.1 Implementation of Model

In order to build a predictive model of the primary drying phase of lyophilization, the equations studied by Pikal and presented in section 2.1.1 were adapted and implemented in the gPROMS FormulatedProducts® custom modelling environment. A user interface was built within the model using XML language

3.2 Model interface

In order to better use this model, a user interface dialog box was constructed where the user can insert the inputs of the model, before running it. In this dialog box, the user have various tabs like the 'Operation and Vial Parameters' tab , the 'Properties' tab, the 'Resistance Parameters' tab and the 'Number of Slices' tab.

In the 'Operation and Vial Parameters' tab, as can be seen in figure 3.1 , the user defines the parameters related to the operation of the lyophiliser like the chamber pressure and the shelf temperature. The user can also define parameters related to the vial, such as vial outer diameter and ratio between vial outer area and vial inner area. Parameters related to the solution specifications, such as fill volume and the concentration of the solute, can also be defined in this tab.

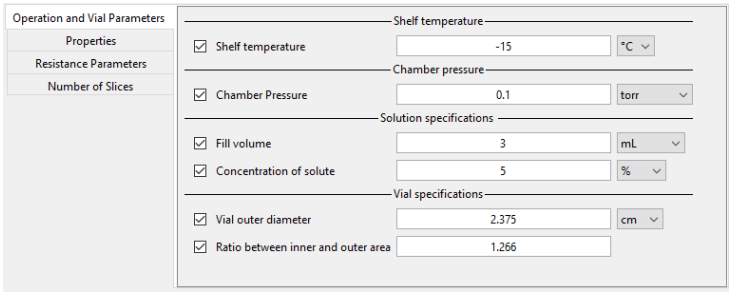

Figure 3.1: gPROMS model interface: Operation and Vial Parameters tab.

In the 'Properties' tab, as can be seen in figure 3.2, the user defines parameters related to the physical properties of the content inside the vial. In this tab, the user defines whether the product remains amorphous when frozen or if the product assumes a crystalline structure. In this tab, the densities of the solution, ice and solute are inserted such as the enthalpy of sublimation ($cal\ g^{-1}$), the effective thermal conductivity of the frozen product ($cal\ cm^{-1}sec^{-1}K^{-1}$) and the vial heat transfer coefficient ($cal\ cm^{2}sec^{-1}K^{-1}$).

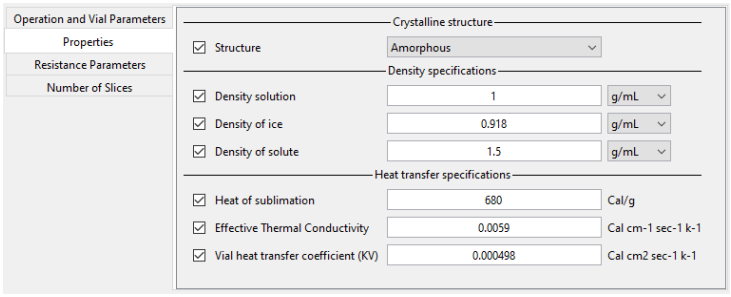

Figure 3.2: gPROMS model interface: Properties Tab.

In the 'Resistance Parameters' tab, as can be seen in figure 3.3, the user defines parameters related to the resistance to the vapour flow of the dried cake such as initial resistance (R_0) and the coefficients A_1 and A_2.

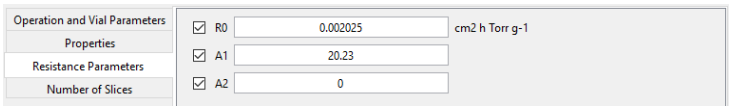

Figure 3.3: gPROMS model interface: Resistance parameters Tab.

In the last tab, 'Number of Slices', as can be seen in figure 3.4, the user defines the number of slices in which the frozen cake will be divided in order to calculate the outcome of the model. This value can range between 2 and 1000 slices. With a bigger number of slices, the model can better describe the evolution of the primary drying phase.

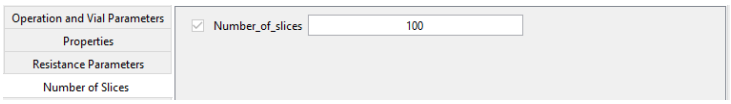

Figure 3.4: gPROMS model interface: Number of slices Tab.

Model reports

After the input parameters are inserted in the model, the user runs the model. After the model stops running, reports of the predictions are available, as a table and as graphics.

The table reports a summary of the key parameters, like the average sublimation rate, the maximum temperature of the product and the total duration of the primary drying. The table can be seen in the Figure 3.5.

Summary of the key parameters .

Name	Value at time 0.00000	Units
Average Sublimation Rate	0.137443	g/h
Max tempererature of product	-22.6889	°C
Total duration	21.9016	h

Figure 3.5: gPROMS model interface: Summary report of the model.

The graphic reports of the model can be seen in Figure 3.6.

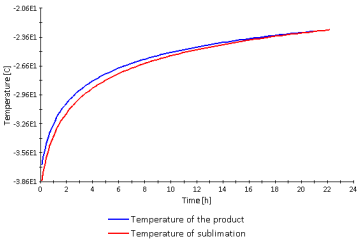

(a) Time course of temperature.

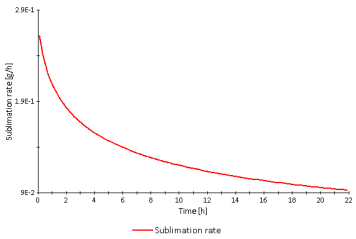

(b) Time course of sublimation rate.

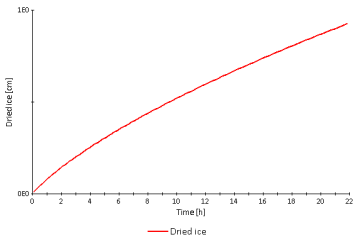

(c) Time course of the dried product length.

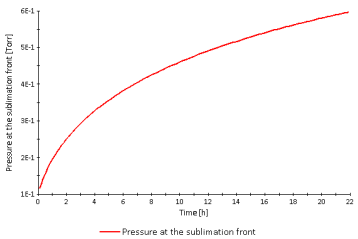

(d) Time course of the sublimation front pressure.

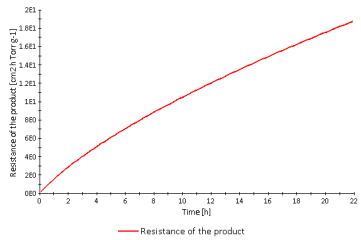

(e) Time course of the resistance of the product.

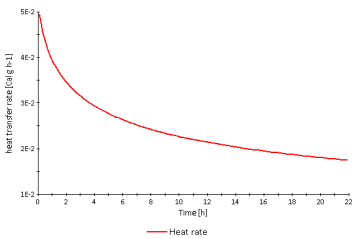

(f) Time course of the heat transfer of the product.

Figure 3.6: gPROMS model interface: Graphic report of the model.

In the first graphic (3.6a), the time course of the temperature of the product and sublimation front temperature are displayed, giving the user an idea of how the different temperatures vary with time. The second graphic (3.6b) shows the time course of the sublimation rate. The third graphic (3.6c) shows how much of the product is dried at each time. The fourth graphic (3.6d), shows the variation of the pressure at the sublimation front with time. The fifth graphic (3.6e) express how the resistance to the vapour flow of the dried product vary with time. The last graphic (3.6f) indicate the heat transferred from the shelf to the frozen product inside the vial.

These graphics provide a visual aid to the user, enhancing the user capability of understanding the process. For example, it is possible to deduce from the graphics that the length of the dried product increases with time, increasing the resistance of the product to mass transfer and therefore the pressure at the sublimation front leading to the reduction of the sublimation rate. The temperature of the product will increases with time, and the heat transfer rate decreases as the temperature of the product approach the shelf temperature, since the driving force is smaller.

3.3 Model validation

In order to validate the model, the results from the model were firstly compared with the results of the LyoModelling calculator from SP Scientific, in order to determine if the model was well implemented in the gPROMS platform. Following this, the results from the model were compared with experimental data, obtained from the work of Wei Y. Kuu (2006), in order to determine if the model was capable of predicting data from a real process.

3.3.1 LyoModelling calculator Comparison

With the purpose of comparing the two models, the same input parameters were put in both models, and various runs were made in both models varying only the concentration of the solute in the solution inside the vial and the structure of the product. The input parameters used in both models are seen in table 3.1 .

Table 3.1: Parameters input used in the comparison between gPROMS steady-state model and the LyoModelling Calculator.

Parameter	Input
Shelf Temperature ($^{\circ}C$) [61]	0
Chamber Pressure ($mTorr$) [61]	25
Fill Volume (mL) [61]	3
Vial Outer Diameter (cm) [61]	2.4
Ratio [61]	1.1
R_0 ($cm^2\ h\ Torr\ g^{-1}$) [61]	1.4
A_1 ($cm\ h\ Torr\ g^{-1}$) [61]	16
A_2 (cm^{-1}) [61]	0
Solution Density ($g\ mL^{-1}$) [62]	1
Ice Density ($g\ mL^{-1}$) [62]	0.918
Solute Density ($g\ mL^{-1}$) [62]	1.5
Heat of Sublimation ($cal\ g^{-1}$) [62]	680
K_i ($cal\ cm^{-1}sec^{-1}K^{-1}$) [62]	5.9×10^{-3}
K_v ($cal\ cm^{-2}sec^{-1}K^{-1}$) [62]	4×10^{-4}
Number of Slices [62]	10

The shelf temperature, chamber pressure, fill volume, vial outer diameter and resistance parameters (R_0, A_1, A_2) were chosen having as base the webinar of SP scientific about the LyoModelling calculator [61]. The remaining parameters are the default values of the LyoModelling calculator [62]. The concentration of the solute in the solution was varied between 0 and 20%, with both product structures being used at each concentration. The comparison between both models can be seen in Table 3.2.

Table 3.2: Results of the comparison between the gPROMS steady-state model and the LyoModelling Calculator.

Concentration (%)	Product structure	Variable	gPROMS model	LyoModelling Calculator	Relative error (%)
0	N/A	Primary Drying Time (h)	12.6	12.5	1
		Average Sublimation Rate (g/h)	0.237	0.233	2
		Max Product Temperature ($^{\circ}$C)	-20.9	-20.9	0
10	Amorphous	Primary Drying Time (h)	11.0	10.9	1
		Average Sublimation Rate (g/h)	0.238	0.234	1
		Max Product Temperature ($^{\circ}$C)	-21.0	-21.0	0
	Crystalline	Primary Drying Time (h)	11.2	11.2	0
		Average Sublimation Rate (g/h)	0.239	0.235	2
		Max Product Temperature ($^{\circ}$C)	-21.1	-21.1	0
20	Amorphous	Primary Drying Time (h)	9.3	9.3	0
		Average Sublimation Rate (g/h)	0.240	0.236	2
		Max Product Temperature ($^{\circ}$C)	-21.2	-21.2	0
	Crystalline	Primary Drying Time (h)	9.9	9.9	0
		Average Sublimation Rate (g/h)	0.241	0.238	1
		Max Product Temperature ($^{\circ}$C)	-21.4	-21.4	0

As can be seen in table 3.2, the difference between both models is insignificant since the relative error of the gPROMS model to the LyoModelling calculator is always below 2%. Although the relative error is indeed small, it still exist and it is bigger in the average sublimation rate. This small difference can be associated to one main factor, being this factor rounding errors between gPROMS and the LyoModelling calculator. Although this small difference exists, it can be assumed that the equations were well implemented on gPROMS.

3.3.2 Experimental data Comparison

In his work, Wei Y. Kuu determined the dry layer mass transfer resistance for various pharmaceutical formulations during primary drying in a laboratory freeze-dryer and validated the 1D steady-state model he created with the product temperature profiles obtained with the experiments. His work is going to be used in the validation, since it had the results of the experiments and the parameters used in the model. However, only the experiment using the 5% mannitol formulation is going to be used, since it is the only formulation where all the parameters are stated [67] .

With the experiment where he used the 5% mannitol formulation, two different vials (Schott and Wheaton vials) were used with slightly different vial heat transfer coefficients (K_v). The product temperature profiles at the bottom of the product were obtained, for each type of vial, by probing 5 centre vials at the bottom with thermocouples, and the product temperature profiles obtained in laboratory were compared to the product temperature profiles obtained in the model [67].

In order to validate the gPROMS model, the bottom product temperature profile of the product will be compared to the product temperature profiles obtained in laboratory for the 5% mannitol formulation. 2 experiments were performed, using the same parameters, but using the two different vial types (Schott and Wheaton vials) with slightly different heat transfer coefficients. The parameters used in the gPROMS model is displayed in table 3.3.

Table 3.3: Parameters input used in the validation of the gPROMS steady state model with experimental data.

Parameter	Values
Shelf Temperature ($^{\circ}C$) [67]	-15
Chamber Pressure ($mTorr$) [67]	100
Fill Volume (mL) [67]	3
Concentration ($\%w/v$) [67]	5
Outer Diameter (cm) [67]	2.375
Ratio between inner and outer area [67]	1.27
Product Structure [67]	Amorphous
Density Solution ($g\ mL^{-1}$) [62]	1
Density Ice ($g\ mL^{-1}$) [62]	0.918
Density Solute ($g\ mL^{-1}$) [62]	1.5
Heat of Sublimation ($cal\ g^{-1}$) [62]	680
K_i ($cal\ cm^{-1}sec^{-1}K^{-1}$) [62]	5.9×10^{-3}
R_0 ($cm^2\ h\ Torr\ g^{-1}$) [67]	2.025×10^{-4}
A_1 ($cm\ h\ Torr\ g^{-1}$) [67]	20.23
A_2 (cm^{-1}) [67]	0
Number of Slices	100
K_v ($cal\ cm^{-2}sec^{-1}K^{-1}$) [67]	4.98×10^{-4} (Schott) 5.13×10^{-4} (Wheaton)

The values for the shelf temperature, chamber pressure, fill volume, concentration, outer diameter, ratio between inner and outer area, product structure, R_o, A_1, A_2 and vial heat transfer coefficient were taken from the Wei. Y. Kuu paper. The values for the density of ice, heat of sublimation and effective thermal conductivity were the default values from the LyoModelling calculator. The density of solute is the tabulated value for mannitol. The density of the solution was estimated to be equal to the density of water, since the concentration of the solute is small.

The graphic comparing the product profiles of gPROMS model, the experimental data for both vials is showed in figure 3.7.

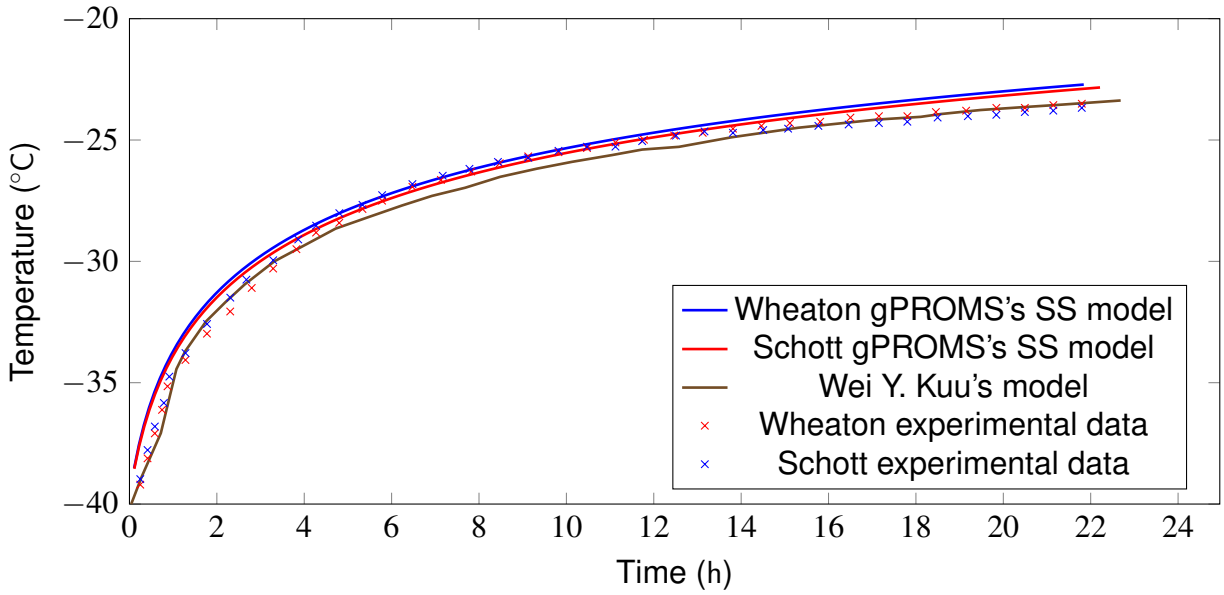

Figure 3.7: Comparison of the product temperature profile between gPROMS steady-state model and experimental data obtained from Wheaton and Schott vials.

By analysing the figure 3.7, it can be observed that, for both vials, the model has a similar temperature profile as the experimental data. Although the profile is similar, the temperature and the total time calculated by the model are slightly superior to the ones obtained experimentally. To further enhance the analysis, the error of the model maximum temperature and total duration relative to the experimental data can be seen in the Table 3.4, for both vials.

Table 3.4: Comparison of the maximum temperature and the total duration of the process between the experimental data and the gPROMS steady-state model, for the Wheaton and Schott vials.

Vial	**Variable**	**Experimental Data**	**gPROMS Model**	**Relative error (%)**
Wheaton	Maximum Temperature (°C)	-23.5	-22.71	3
	Total Duration (h)	21.80	21.84	0
Schott	Maximum Temperature (°C)	-23.68	-22.83	3
	Total Duration (h)	21.80	22.21	2

As it can be seen in Table 3.4 , the relative error between the model and the experimental data is below 3% for the maximum temperature of the primary drying and the total duration in both vials, showing a good agreement between experimental data and the model.

3.4 Global system analysis (GSA) study

After the validation of the model, is important to understand how certain key parameters affect the output of the model. In order to have that understanding, a sensitivity analysis using the Global system analysis (GSA) tool was performed.

The GSA tool allows the user to perform an uncertainty analysis or a sensitivity analysis. The sensitivity analysis in gPROMS® is the study of how the variance of the model output depends on the input factors that are affected by uncertainty. The variance-based sensitivity analysis measure the influence of individual factors on the model output [68, 69].

When interpreting the sensitivity indices, the first-order effect index (S_i) and the total effect index (S_{Ti}) need to be taken in account. The S_i represents the main effect contribution of each input factor to the variance of the output. The higher the value of S_i, the higher the influence factor on the output, and a $S_i = 0$ indicates that the factor has no direct influence on the output, however it can still be an important factor through it is interaction with other factors.The sum of all S_i is always equal or lower to 1, and if it is equal to 1 then there are no interaction between the factors [68, 69].

The total effect index (S_{Ti}) accounts for the total contribution to the output variance of the i_{th} factor, including its individual contribution (first-order effect) plus all higher-order effects due to its interaction with other factors. S_{Ti} must be equal or higher to S_i and if its equal, then the factor has no interaction with other factors. If $S_{Ti} = 0$, the factor has no influence in the model output. The sum of all S_{Ti} is always equal or higher than 1, and if it is equal to 1 then there are no interaction between the factors [68, 69].

The influence of parameters, such as the vial heat transfer coefficient, the initial resistance, shelf temperature and were tested on the maximum temperature of product and the total duration of the primary drying. The GSA simulated the model thousands of times, varying the A_1, K_v and the chamber pressure between stipulated bounds, that can be seen in Table 3.5

Table 3.5: Parameters bounds used in the global system analysis (GSA) study

Parameter	Lower Bound	Upper Bound
A_1 (Resistance)	10^{-12}	500
K_v ($cal\ cm^{-2}sec^{-1}K^{-1}$)	10^{-20}	0.01
Chamber Pressure (Torr)	0	0.5

The GSA provided sensitivity indices, which indicates which of the parameters have more influence on the output (total duration and maximum product temperature) of the model. The sensitivity indices of 1st order and total effect are showed in Table 3.6.

Table 3.6: Global system analysis results: sensitivity analysis factors

Parameter	Maximum Temperature		Total Duration	
	1^{st} order effect	Total effect	1^{st} order effect	Total effect
K_v	0.404	0.795	0.032	0.045
Resistance	0.148	0.641	0.882	0.902
Chamber Pressure	-0.008	0.032	0.056	0.083

As it can be seen, K_v has the most direct influence in the maximum temperature amongst the parameters studied because it has the biggest 1st order effect, and has a lot of influence in other parameters that also influence the maximum temperature, as it is showed by it is high value of total effect. Although having a huge influence in the maximum temperature, it is influence in total duration is minimum, compared to the other parameters studied.

The resistance has a small direct influence in the maximum temperature but it has a big effect on other parameters that influence the maximum product temperature and it is almost the only parameter of the three that affects the total duration.

The chamber temperature is the parameter amongst the three studied that least affect both maximum product temperature and the total duration of the process. The 1st order effect is insignificant, being practically 0 for the maximum temperature.

With this study, is possible to show how much influence certain parameters have in the output of the process, but it is not possible to know how this parameters influence said outputs. In order to do this, a different study was performed, using the GSA, where the K_v was ranged from 10^{-20} to 0.1 ($cal\ cm^{-2}sec^{-1}K^{-1}$), and the maximum temperature of the process was reported, at different shelf temperatures. The results can be seen in Fig 3.8.

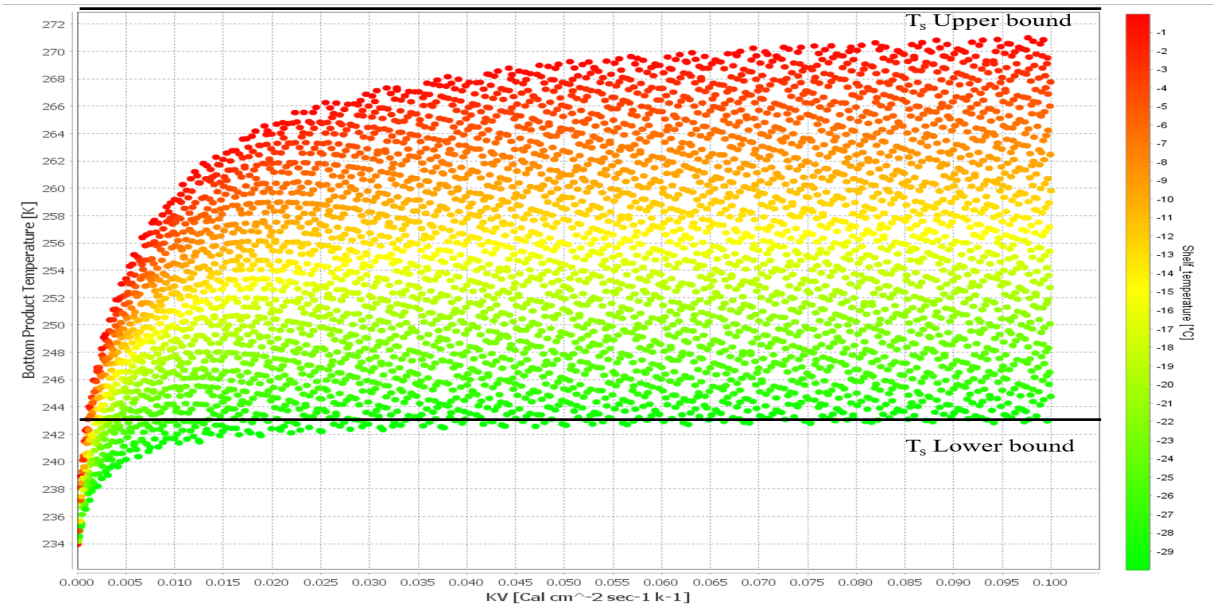

Figure 3.8: Global system analysis results: Vial heat transfer coefficient influence in maximum temperature of the product at different shelf temperatures.

As it can be seen, at a fixed shelf temperature, the maximum product temperature will increase with the increase of the K_v, until it reaches the shelf temperature. When the maximum product temperature reaches the shelf temperature, it does not surpass it, even if the K_v is further increased because when this happens, the driving force (difference between the shelf temperature and product temperature) is zero and the temperature do not increase any further. This behaviour can be verified by the fact that the processes that use the lower and upper shelf temperature bounds tend to said shelf temperatures. The bottom product temperature of the process with the lower shelf temperature reaches said temperature faster than the process with the upper shelf temperature bound, precisely because the shelf temperature is lower and if the K_v was further increased, the bottom product temperature of process with the upper shelf temperature bound would eventually reach the shelf temperature upper bound.

A similar study was performed to the Resistance in which it was ranged from 10^{-12} to 100 , but instead of analysing the maximum temperature of the product at different shelf temperatures, the total duration of the process was analysed. The results can be seen in Figure 3.9.

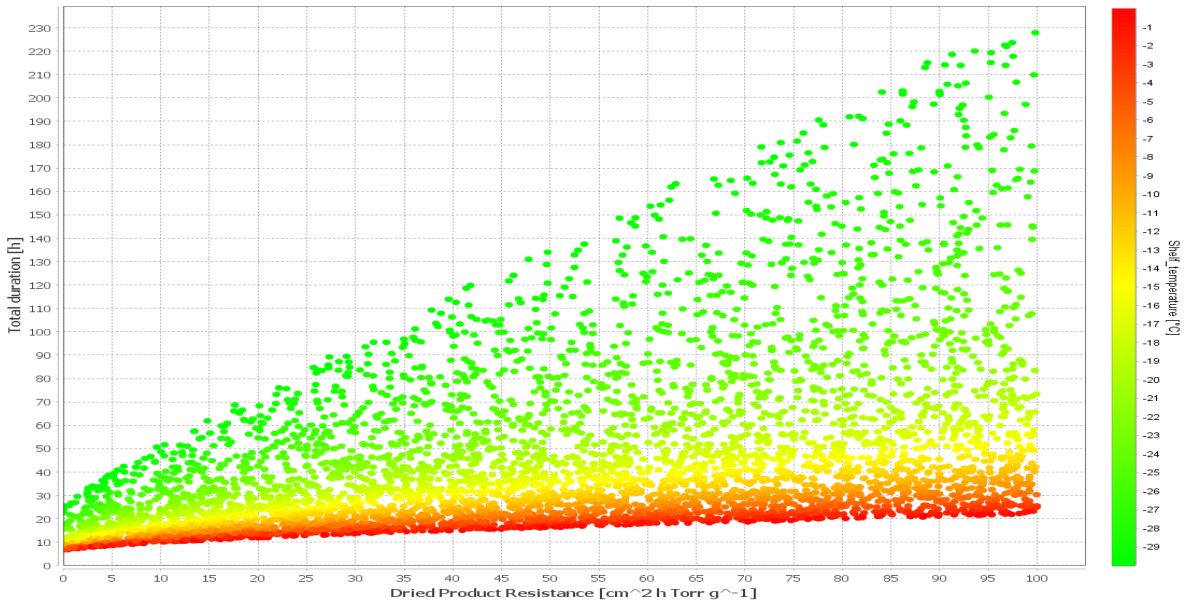

Figure 3.9: Global system analysis results: Resistance influence in total duration of the process at different shelf temperatures.

When analysing the Figure 3.9, it can be observed that at low shelf temperatures, an increase in the resistance originates a big increase of the total duration of the process, but at high shelf temperatures, big increases in the resistance do not affect the duration of the process that much. In order to understand this, is necessary to do another study. Four more simulations were made, using the same parameters as before, but varying in each simulation the shelf temperature and the resistance (A_1). The four simulations are the extreme cases in the GSA study depicted in Figure 3.9. The first simulation is with a shelf temperature of 0 ° C and a resistance (A_1) of 10^{-10} $cm\ h\ Torr\ g^{-1}$ (Case 1). The second simulation is made with a shelf temperature of 0 ° C and a resistance (A_1) of 100 $cm\ h\ Torr\ g^{-1}$ (Case 2). In the third simulation, a lower shelf temperature of -30 ° C and a resistance (A_1) of 10^{-10} $cm\ h\ Torr\ g^{-1}$ were used (Case 3). The last simulation was performed with a shelf temperature of -30 ° C and a resistance (A_1) of 100 $cm\ h\ Torr\ g^{-1}$ (Case 4). The summary of the parameters used can be seen on Table 3.7 and the results of the four cases can be seen in Figure 3.10.

Table 3.7: Summary of the parameters used in the extreme cases on the global system analysis study.

Case	Shelf Temperature ($^{\circ}C$)	A1 ($cm\ h\ Torr\ g^{-1}$)
1	0	10^{-10}
2	0	100
3	-30	10^{-10}
4	-30	100

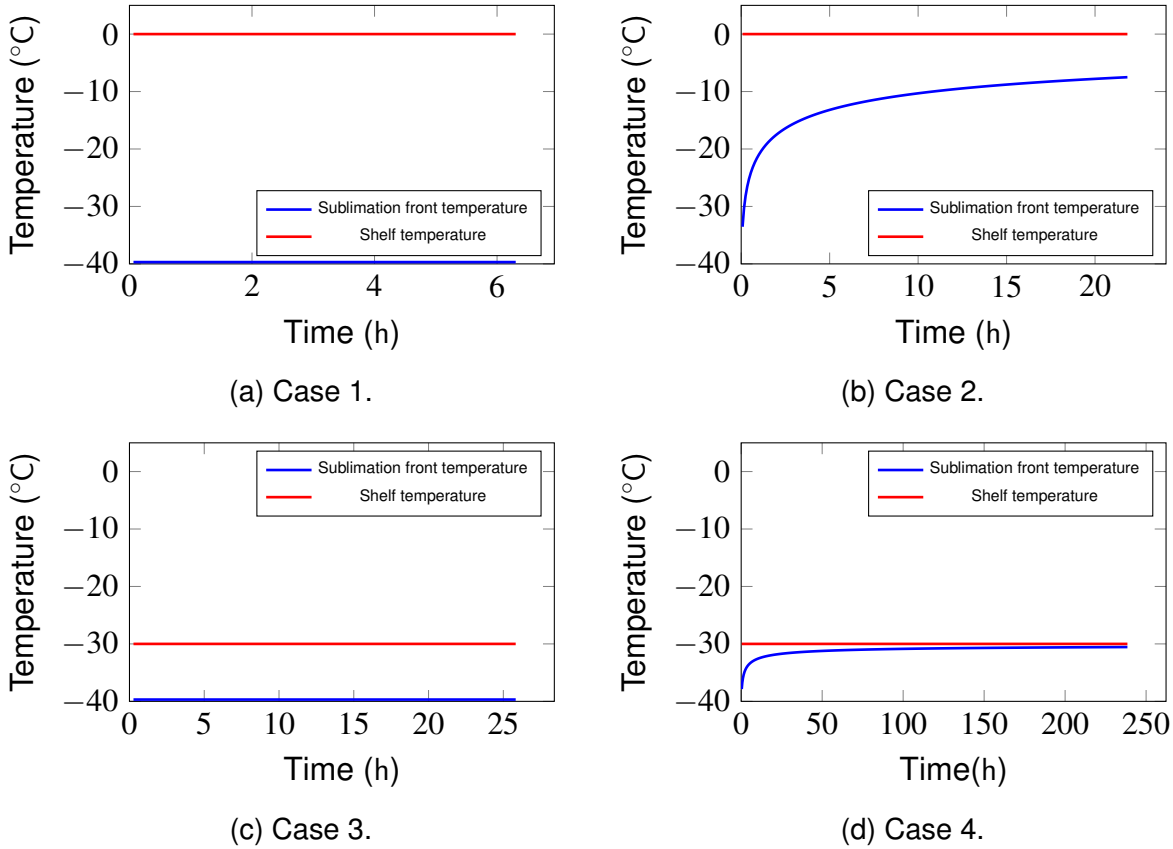

(a) Case 1.

(b) Case 2.

(c) Case 3.

(d) Case 4.

Figure 3.10: Product temperature profiles of the extreme cases on the global system analysis study.

In case 1 the resistance to mass transfer is negligible, resulting in a mass transfer of water almost instantaneous. When this happens, the pressure inside the product is equal to the pressure of the chamber and the temperature of the sublimation front do not change from the beginning of the process. This results in a huge driving force (difference between the shelf temperature and product temperature) for the sublimation to occur, resulting in a fast process.

In case 2 the resistance is high and in this conditions, the temperature of the sublimation front will increase, reducing the driving force for the sublimation. But because

the shelf temperature is high, the driving force is still high, despite the resistance to mass transfer being big. This explains why at high shelf temperatures, a big increase in the resistance produce a small increase in total duration of the process.

In case 3 the resistance is again negligible, but the shelf temperature is lower, resulting in a smaller driving force, leading to a longer process that in the previous cases.

In Case 4 the resistance is high, resulting in a increase of the sublimation front temperature, until it reaches the shelf temperature. Because of the low value of the shelf temperature, the driving force is minuscule, leading to a process of more than 200 hours. This helps to explain why at low shelf temperatures, a small increase of the resistance results in a big increase of the duration of the process.

This indicates that although the resistance of the product to mass transfer is important to the duration, the shelf temperature plays a bigger role when determining the total duration of the process, as it was already common knowledge in the industry.

Chapter 4

Case Study

A case study was performed in order to compare the 1D steady state model and the 1D dynamic model implemented in gPROMS. This was made in order to compare the strengths and limitations of each model.In order to do that, the predictive and the optimisation capabilities of both models were compared with each other, using the parameters and data from the work of Wei Y. Kuu [67]. A study of how much the temperature ramp of the 1D dynamic model influence the output is also made, in order to understand if this addition to the model has a big influence in key parameters, such as the total duration when compared to the output of the steady-state model

4.1 1D dynamic model

The 1D dynamic model is a model for the primary drying step in a single vial, that was previously implemented in the gPROMS platform. The model is based on the equations reviewed on section 2.1.2, but instead of assuming a tray, it assumes the process occurs in a single vial.

This model differs from the steady-state model for the fact that it allows the simulation of different shelf temperatures profiles, instead of using a constant shelf temperature. Strictly speaking, the model allows to determine the time it takes to the shelf temperature to go from a certain value (fixed by the user) to another, which is called a temperature ramp. It is possible to determine various sequential temperature ramps in the same process, in order to design the shelf temperature profile.

4.2 Predictive capabilities comparison

In order to compare the predictive capabilities, the same inputs were used in both models, being the same that was used on the validation of the steady-state model and the values can be seen on table 3.3. In this study only the Shott vials were taken

in account, because the temperature profile of both vials (Wheaton and Schott) are similar. In the dynamic model, two runs of the process were made, one with a ramp temperature of 1 hour as it was used in the experimental process, and other without the ramp temperature. The results can be observed in the figure 4.1.

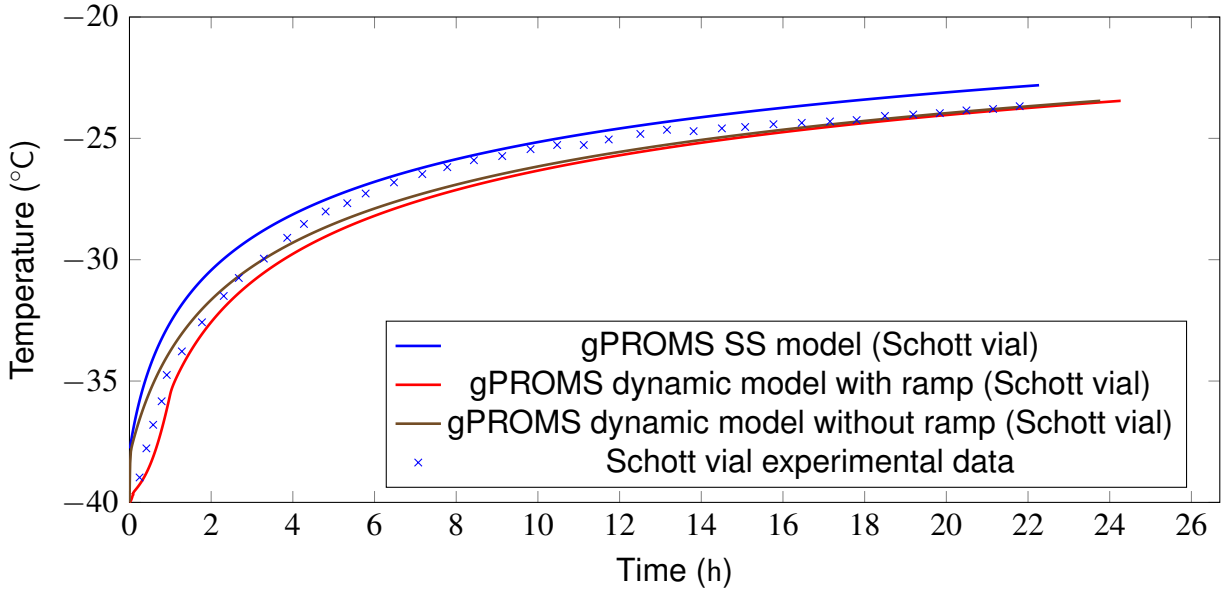

Figure 4.1: Comparison between the product temperature profiles of the gPROMS steady-state model, gPROMS 1D dynamic model, and experimental data for Schott vials

By analysing the Figure 4.1, it can be observed that the product temperature profile of the steady-state model (SS model) and the dynamic model (USS model) are similar, being both able to predict with some accuracy the product temperature profile of the experimental data. Despite both being able to predict accurately, the steady state model predicted a duration closer to the experimental data, and the dynamic model was able to predict more accurately the temperature at the end of the primary drying stage.

Regarding the simulation with the ramp, it predicts a longer process duration than the same process without the ramp, as it was expected. In the initial stages of the primary drying, the product temperature profile differs from the process with and without the ramp. It can be seen that in the process with the ramp, the increase in the temperature of product is slower compared with the same process but without ramp. In the second half of the process, the profiles in both cases are the same, predicting the same final temperature. This indicates that the influence that the temperature ramp has in the maximum temperature of the product is negligible, but it has influence in the total duration of the process and this influence is going to be further studied.

4.3 Temperature ramp study

In order to study the influence of the shelf temperature ramp, a GSA was was performed in the dynamic model in the same process as was used before, varying the ramp increase rate from 0.1 to 1°C/min. For each ramp increase rate, the total duration of the process was obtained and the deviation of the total duration to the steady-state model was calculated and the results can eb seen in Figure 4.2.

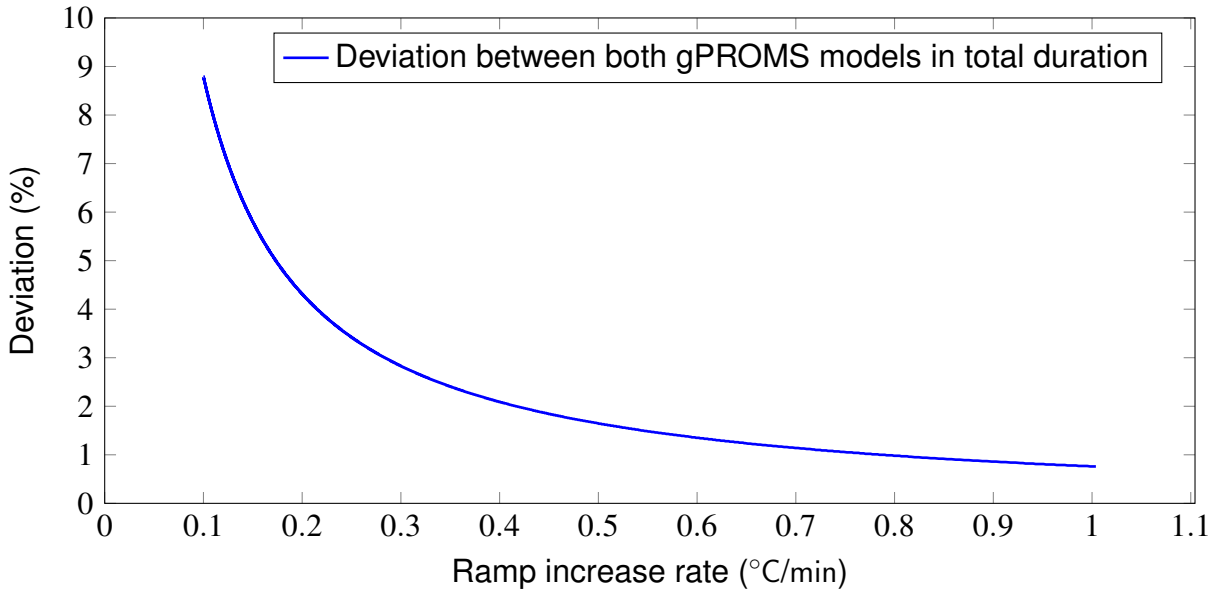

Figure 4.2: Influence of the temperature ramp in the total duration of the process

As it can be seen in Figure 4.2, at high increase rates (fast ramps) the deviation to the steady-state model is minimum, being near 1%, indicating that when the ramp is fast enough, the duration predicted by the dynamic model is close to the duration predicted by the steady-state model. At slow increase rates (slow ramps), the deviation increases to values near 9% indicating that when the ramp is slow enough, the duration predicted by the dynamic model begins to differ significantly from the duration predicted in the steady-state model.

4.4 Optimisation

The optimisation of the primary drying step is crucial in order to obtain better, shorter and cheaper processes. In order to have better processes, it is necessary to understand which model can be better used to optimise a real lyophilization process. In order to do that, both models were used to optimise the process used previously from the work of Wei Y. kuu, using the optimisation tool of gPROMS®. The objective of the optimisation was to minimise the duration of the process, without letting the temperature of the

product surpass -20°C. Although it is not the real collapse temperature for mannitol, it was assumed as it in order to test the optimisation capabilities of both models. In order to do this, the only parameter that was changed in both models was the shelf temperature profile. The optimisation using the steady-state model is shown in Figure 4.3.

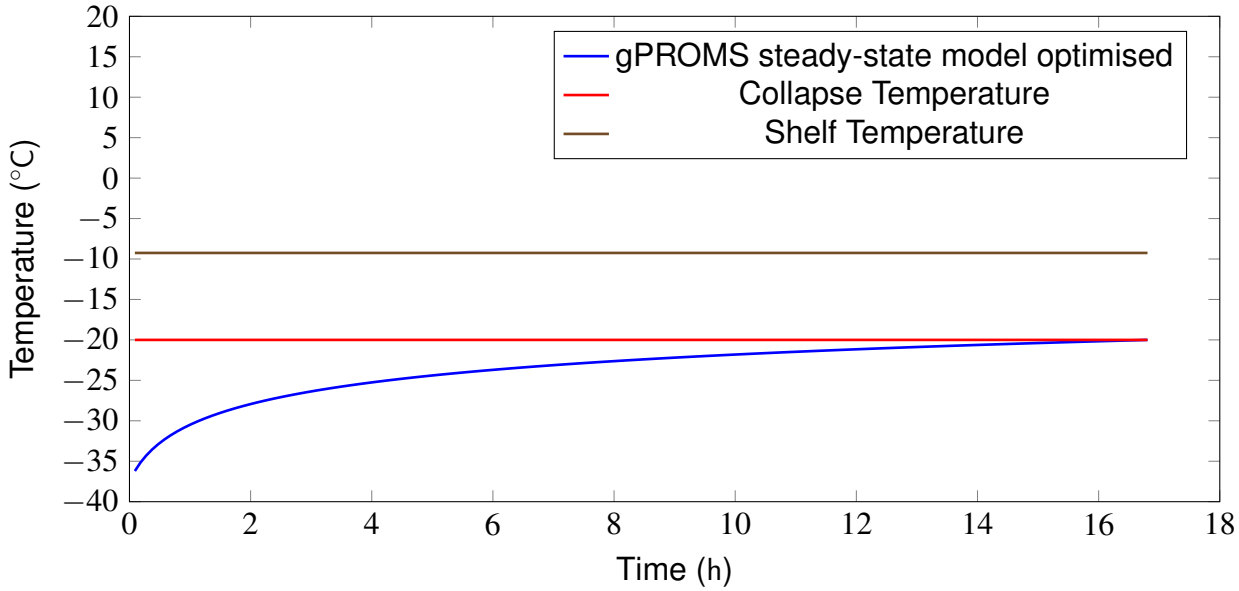

Figure 4.3: Product temperature profile of the process optimised using the gPROMS steady-state model

In the optimisation using the steady-state model, a constant shelf temperature of -9.25°C was obtained, and it resulted in a reduction of nearly 5 hours compared to the prediction before the optimisation, to a total of almost 17 hours. The optimisation using the dynamic model is shown in the Figure 4.4.

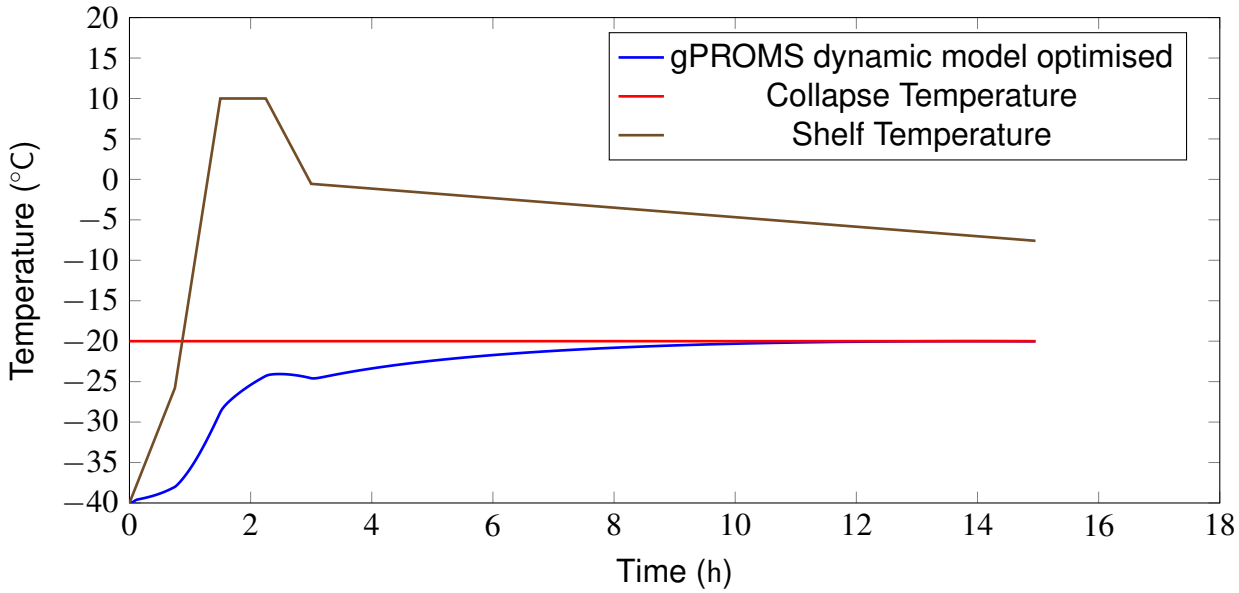

Figure 4.4: Product temperature profile of the process optimised using the gPROMS 1D dynamic model

In the optimisation using the dynamic model, a shelf temperature profile was obtained instead of a constant shelf temperature, and the shelf temperature profile can be seen in Table 4.1.

Table 4.1: Shelf Temperature profile obtained in the optimisation using the 1D dynamic model

Ramp	**Temperature (°C)**	**Ramp duration (min)**
1	-25.79	45
2	10.00	45
3	10.00	45
4	-0.55	45
5	-7.59	End

With this shelf temperature profile, a process duration of almost 15 hours were obtained, resulting in a reduction of almost 9 hours regarding the previous prediction of the original process with this model. The comparison between the total duration of the optimised process with both models can be seen in the Table 4.2.

Table 4.2: Total duration of the process obtained in the 1D steady-state and dynamic models optimised

	USS model optimised	**SS model optimised**
Duration (h)	14.96	16.81

When it comes to the optimisation capability, the steady-state model is able to find a shelf temperature in which the temperature of the product do not surpass the collapse temperature defined, having a big reduction on the process duration, but when comparing with the dynamic model, gPROMS was able to find a more efficient shelf temperature profile, in which the temperature of the shelf is raised to high values in the beginning, increasing the sublimation rate, and then being proceeded by a decrease in the shelf temperature to avoid the temperature of the product to surpass the collapse temperature. This shelf temperature profile allows for a further decrease of the total duration of the process, compared to the steady-state model.

Despite the fact that it provided a faster process, the shelf temperature profile is not practical to be used in a real lyophilization cycle, mainly because the slow decrease of temperature in the last 12 hours. In order to be a practical shelf temperature profile, it is better to have a constant shelf temperature in the last hours of the primary drying step. Using the shelf temperature profile obtained in the optimisation with gPROMS®, a more practical shelf temperature profile was obtained, and it can be seen in the Table 4.3.

Table 4.3: Practical shelf temperature profile obtained in the optimisation using the 1D dynamic model

Ramp	**Temperature (°C)**	**Ramp duration (min)**
1	-25.8	45
2	18.0	60
3	18.0	45
4	-7.8	45
5	-7.8	End

With this shelf temperature profile, we obtained the product temperature profile depicted in the Figure 4.5.

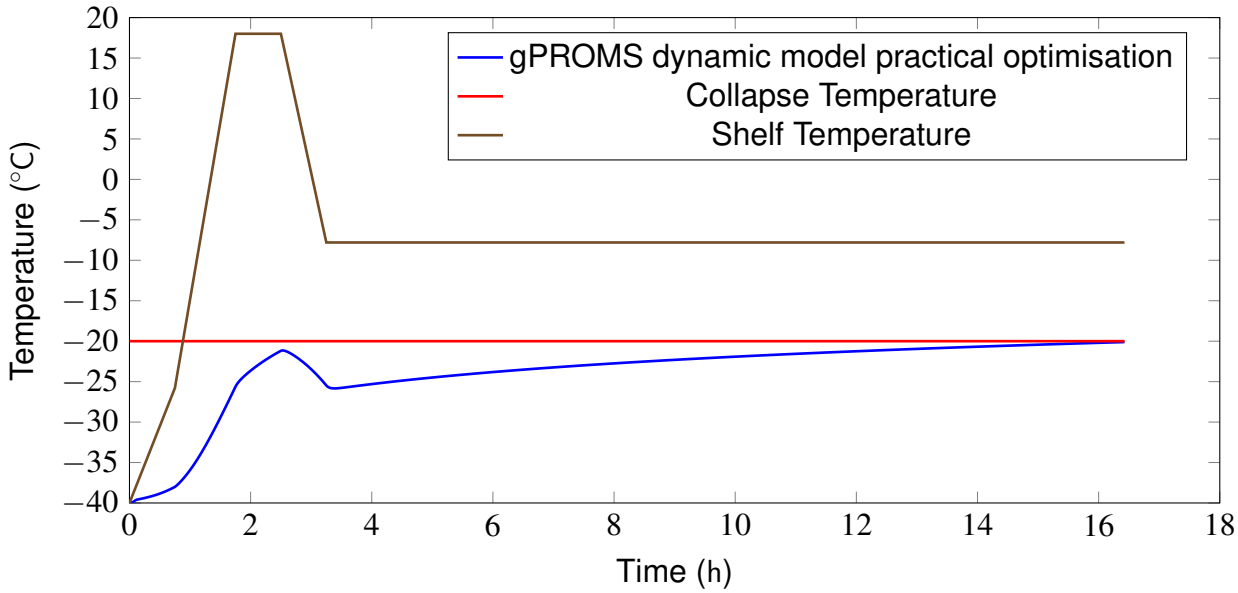

Figure 4.5: Product temperature profile of the process optimised using a practical shelf temperature profile

In the Figure 4.5, it can be seen that the process using the practical shelf temperature profile is almost 1.5 hours longer than the one obtained using the gPROMS® optimisation tool, but this process is easier to apply to a real lyophilization cycle. Using this cycle, a reduction of 7.5 hours is obtained, when comparing with the previous prediction of the original process with the dynamic model. The comparison between the duration of the practical process design with the steady-state model optimised is showed in the Table 4.4.

Table 4.4: Practical shelf temperature profile obtained in the optimisation using the 1D dynamic model

	Practical design optimisation	**SS model optimised**
Duration (h)	16.42	16.81

When comparing this practical process design with the steady-state model optimised, the duration of both processes are similar, being the process with the practical design only 20 minutes shorter. This is a small difference, but in a real process, it is impossible to use the process described in the steady-state model, because it assumes a constant temperature from the beginning of the primary drying step, but at the beginning of the step, the shelf temperature starts at the temperature in which the freezing steps end. With this said, the steady-state model is not the best for the optimisation of a process, because the process described is not possible to be used in practice.

Chapter 5

Conclusion

In this work, a mathematical model for the primary drying of the lyophilization process was implemented, validated and studied.

A predictive model for the primary drying step, with access to all of the gPROMS functionalities was successfully built, having as well a user-friendly interface and a graphic report of the results, allowing for a model that is easy to use analyse the results.

The model was successfully validated by comparing it with the LyoModelling Calculator output. It was possible to conclude that the model implemented in gPROMS can provide the same results as the LyoModelling calculator, and it has the advantage of having the gPROMS® tools, such as the Global System Analysis and the optimisation tools.

When the model was successfully validated using experimental data obtained from an article, it was concluded that the model was able to predict, with a good accuracy, the product temperature profile of a real lyophilization process.

Moreover, a sensitivity analysis was performed in order to analyse the influence of certain key parameters, such as the resistance to mass transfer, chamber pressure and vial heat transfer coefficient, using the GSA tool of gPROMS®. This tool allowed the run of thousands of simulations where the key parameters were varied between defined bounds, and the influence it had on the output was determined. With the sensitivity analysis, it was possible to determine that between the key parameters studied, the vial heat transfer coefficient had the most influence on the maximum product temperature and the resistance to mass transfer had the most influence in the total duration.

Finally, the model was compared with a more complex model (1D dynamic model) that was previously implemented on gPROMS®, with the capability of simulating various shelf temperature ramps. When this capability was studied, it was concluded that the temperature ramp had little effect in the maximum product temperature predicted by the 1D dynamic model, but it had influence in the total duration of the process, especially when the temperature ramp that was used had a slow increase rate, resulting in longer processes compared with the steady-state model implemented in gPROMS®.

The predictive and optimisation capabilities of the steady-state model were compared with the 1D dynamic model. Regarding the predictive capability, the two models are similar, with the steady-state model being better at predicting the duration of the process and the 1D dynamic model being better at predicting the maximum temperature. When it comes to the optimisation capabilities though, it was concluded that the steady-state model implemented in gPROMS® is not as good as the 1D dynamic model at optimising the primary drying step of lyophilization.

In conclusion, the predictive model implemented can be used in the initial steps of the development of a lyophilization process, in order to have an estimate of the duration and the product temperature profile, but when it comes to the optimisation, this model can be used but it is not the most suited for it, because it is impossible to apply the shelf temperature profile provided in a real process.

5.1 Future Work

Regarding the steady-state model implemented in gPROMS®, it is recommended to test it even further, using different processes and real data. It is also recommended to compare the model with a even more complex model (two-dimensional dynamic model) in order to better understand the strengths and limitations of the model.

It is also important to implement a model for the freezing step, since there are no software available able to predict this step. With this model implemented, it would be possible to predict the size of the pores in the product and consequently, the resistance to mass transfer of the product. This would also allow to, together with the models for the primary and secondary steps, design the whole process from the beginning to end.

Bibliography

[1] D. Bhambere, "Lyophilization / Freeze Drying – A review," *World Journal of Pharmaceutical Research*, vol. 4, no. 8, pp. 516–543, 2016.

[2] A. Shanley, "Modernizing Lyophilization," *BioPharm International*, vol. 30, no. 12, pp. 50–52, 2017.

[3] A. G. Ogienko, V. A. Drebushchak, E. G. Bogdanova, and A. S. Yunoshev, "Thermodynamic Aspects of Freeze-drying: A Case Study of an "Organic Solvent–water" System," *Journal of Thermal Analysis and Calorimetry*, vol. 127, no. 2, pp. 1593–1604, 2017.

[4] S. Chandrasekhar and E. M. Topp, "Thiol-Disulfide Exchange in Peptides Derived from Human Growth Hormone during Lyophilization and Storage in the Solid State," *Journal of Pharmaceutical Sciences*, vol. 104, no. 4, pp. 1291–1302, 2015.

[5] F. Franks and T. Auffret, "Freeze-drying of Pharmaceuticals and Biopharmaceuticals." RSCPublishing, 2007, vol. 1, pp. 1–53.

[6] S. P. Ishwarya, "Spray-freeze- drying : A Novel Process for the Drying of Foods and Bioproducts," *Trends in Food Science & Technology*, vol. 41, no. 2, pp. 1–21, 2014.

[7] K. Debus, "Lyophilization Experiences Growth Spurt in Pharma," *Pharmaceutical Processing*, vol. 32, no. Setptember/October, pp. 22–24, 2017.

[8] D. Varshney and M. Singh, "History of Lyophilization," in *Lyophilized Biologics and Vaccines*. Springer, 2015, ch. 1, pp. 3–10.

[9] J. G. Day and M. R. McLellan, *Cryopreservation and Freeze-drying Protocols*, 2nd ed., J. G. Day and G. N.Stacey, Eds. Humana Press, 1995, vol. 38.

[10] H. Tse Chao, L. Bao Lin, and Z. Hua, "Freeze drying of pharmaceutical and food products." Woodhead Publishing, 2010, pp. 1–54.

[11] A. Bissoyi, A. Kumar, and A. Rizvanov, “Recent Advances and Future Direction in Lyophilisation and Desiccation of Mesenchymal Stem Cells,” *Stem Cells International*, vol. 2016, 2016.

[12] S. S. Buchanan, D. W. Pyatt, and J. F. Carpenter, “Preservation of Differentiation and Clonogenic Potential of Human Hematopoietic Stem and Progenitor Cells during Lyophilization and Ambient Storage,” *PLoS ONE*, vol. 5, no. 9, pp. 1–11, 9 2010.

[13] P. Loi, K. Matsukawa, and G. Ptak, “Freeze-Dried Somatic Cells Direct Embryonic Development after Nuclear Transfer,” *PLoS ONE*, vol. 3, no. 8, pp. 1–6, 8 2008.

[14] M. Zhang, H. Oldenhof, and B. Sydykov, “Freeze-drying of Mammalian Cells Using Trehalose: Preservation of DNA Integrity,” *Scientific Reports*, vol. 7, no. 1, pp. 1–10, 2017.

[15] A. Kharaghani, “Freeze-Drying,” in *Ullmann’s Encyclopedia of Industrial Chemistry*. Wiley-VCH, 2017.

[16] M. Pikal, M. Roy, and S. Shah, “Mass and Heat Transfer in Vial Freeze Drying of Pharmaceuticals: Role of the Vial,” *Pharm. Sci.*, vol. 73, p. 1224–1237, 1984.

[17] A. Liapis and R. Litchfield, “Numerical Solution of Moving Boundary Transport Problems in Finite Media by Orthogonal Collocation,” *Chemical Engineering Science*, vol. 3, pp. 615–621, 1979.

[18] R. Litchfield, “Optimal Control of a Freeze Dryer,” *Chemical Engineering Science*, vol. 34, no. 7, pp. 975–981, 1979.

[19] M. J. Pikal and W. J. Mascarenhas, “The nonsteady state modeling of freeze drying: In-process product temperature and moisture content mapping and pharmaceutical product quality applications,” *Pharmaceutical Development and Technology*, vol. 10, no. 1, pp. 17–32, 2005.

[20] K. Nakagawa, “Modeling of Freezing Step During Freeze-Drying of Drugs in Vials,” *AIChE Journal*, vol. 53, no. 5, pp. 1362–1372, 2007.

[21] LyoHub, “Technology Roadmap,” 2017, https://pharmahub.org/groups/lyo/lyohub_roadmapping, accessed on 2018-09-04.

[22] G.-W. Oetjen, “Freeze-Drying,” in *Ullmann’s Encyclopedia of Industrial Chemistry*. Wiley-VCH, 2012, pp. 52–100.

[23] V. Koganti, S. Luthra, and M. J. Pikal, “The Freeze-drying process: The use of mathematical modeling in process design, understanding, and scale-up,” in *Chemical Engineering in the Pharmaceutical Industry: R&D to Manufacturing*, D. Ende, Ed. John Wiley & Sons, Inc., 2010, ch. 41.

[24] P. Fonte, P. R. Lino, V. Seabra, A. J. Almeida, S. Reis, and B. Sarmento, “Annealing as a Tool for the Optimization of Lyophilization and Ensuring of the Stability of Protein-loaded PLGA Nanoparticles,” *International Journal of Pharmaceutics*, vol. 503, no. 1-2, pp. 163–173, 2016.

[25] W. Y. Kuu, K. R. Obryan, L. M. Hardwick, and T. W. Paul, “Product Mass Transfer Resistance Directly Determined During Freeze-drying Cycle Runs Using Tunable Diode Laser Absorption Spectroscopy (TDLAS) and Pore Diffusion Model,” *Pharmaceutical Development and Technology*, vol. 16, no. 4, pp. 343–357, 2011.

[26] W. Y. Kuu, M. J. Doty, E. Nisipeanu, C. L. Rebbeck, Y. K. Cho, and M. H. Smit, “Modeling of Heat and Mass Transfer Processes for the Gap-lyophilization System Using the Mannitol-trehalose-NaCl formulation,” *Journal of Pharmaceutical Sciences*, vol. 103, no. 9, pp. 2784–2796, 2014.

[27] X. Lu and M. J. Pikal, “Freeze-Drying of Mannitol-Trehalose-Sodium Chloride-Based Formulations: The Impact of Annealing on Dry Layer Resistance to Mass Transfer and Cake Structure,” *Pharmaceutical Development and Technology*, vol. 9, no. 1, pp. 85–95, 2004.

[28] M. J. Pikal and S. Shah, “The Collapse Temperature in Freeze Drying: Dependence on Measurement Methodology and Rate of Water Removal from the Glassy Phase,” *International Journal of Pharmaceutics*, vol. 62, no. 2-3, pp. 165–186, 1990.

[29] X. C. Tang and M. J. Pikal, “Design of Freeze-Drying Processes for Pharmaceuticals: Practical Advice,” *Pharmaceutical Research*, vol. 21, no. 2, pp. 191–200, 2 2004.

[30] R. Pisano, D. Fissore, and A. A. Barresi, “Quality by Design in the Secondary Drying Step of a Freeze-Drying Process,” *Drying Technology*, vol. 30, no. 11-12, pp. 1307–1316, 2012.

[31] J. Barley, “Basic Principles of Freeze Drying,” pp. 1–14, 2009, https://www.spscientific.com/freeze-drying-lyophilization-basics/, accessed on 2018-09-04.

[32] M. Dellinger, “Basic Lyophilizer Maintenance Helps Assure Good Results,” pp. 1–6, 2009.

[33] Millrock Technology, “How to Choose a Lyophilizer,” https://www.millrocktech.com/lyosight/how-to-choose-a-lyophilizer/, accessed on 2018-09-04.

[34] A. A. Barresi, V. Rasetto, and D. L. Marchisio, “Use of Computational Fluid Dynamics for Improving Freeze-dryers Design and Process Understanding. Part 1: Modelling the Lyophilisation Chamber,” *European Journal of Pharmaceutics and Biopharmaceutics*, vol. 129, pp. 30–44, 2018.

[35] J. Sprung, “Maintaining Your Freeze dryer and Vacuum Pump,” 2014, https://www.labconco.com/articles/maintaining-your-freeze-dryer-and-vacuum-pump, accessed on 2018-09-04.

[36] C. Reiter, “Manifold Freeze Dryers – An Overview of Their Use, Limitations and Some Helpful Hints,” https://www.millrocktech.com/lyosight/lyobrary/tech-notes/, accessed on 2018-09-04.

[37] IMA Life, “Lyomax Series,” https://ima.it/pharma/wp-content/uploads/sites/2/2017/02/LYOMAX_EN.pdf, accessed on 2018-09-04.

[38] FDA, “Guidance for Industry PAT: A Framework for Innovative Pharmaceutical Development, Manufacuring, and Quality Assurance,” *FDA official document*, no. September, p. 16, 2004.

[39] J. G. Rosas, H. de Waard, T. De Beer, C. Vervaet, J. P. Remon, W. L. Hinrichs, H. W. Frijlink, and M. Blanco, “NIR spectroscopy for the in-line monitoring of a multicomponent formulation during the entire freeze-drying process,” *Journal of Pharmaceutical and Biomedical Analysis*, vol. 97, pp. 39–46, 2014.

[40] T. De Beer, P. Vercruysse, and A. Burggraeve, “In-Line and Real-Time Process Monitoring of a Freeze Drying Process Using Raman and NIR Spectroscopy as Complementary Process Analytical Technology (PAT) Tools,” *International Journal of Drug Development and Research*, vol. 98, no. 9, pp. 3430–3446, 2009.

[41] D. Fissore, S. A. Velardi, and A. A. Barresi, “In-line Control of a Freeze-drying Process in Vials,” *Drying Technology*, vol. 26, no. 6, pp. 685–694, 2008.

[42] S. Corbellini, M. Parvis, and A. Vallan, “In-Process Temperature Mapping System for Industrial Freeze Dryers,” vol. 59, no. 5, pp. 1134–1140, 2010.

[43] S. Schneid and H. Gieseler, “Evaluation of a New Wireless Temperature Remote Interrogation System (TEMPRIS) to Measure Product Temperature During Freeze Drying,” *AAPS PharmSciTech*, vol. 9, no. 3, pp. 729–739, 2008.

[44] S. Bosca, A. A. Barresi, and D. Fissore, “Use of Soft Sensors to Monitor a Pharmaceuticals Freeze-drying Process in Vials,” *Pharmaceutical Development and Technology*, vol. 19, no. 2, pp. 148–159, 2014.

[45] H. Gieseler, T. Kramer, and M. J. Pikal, “Use of Manometric Temperature Measurement (MTM) and SMART^{TM} Freeze Dryer Technology for Development of an Optimized Freeze-drying Cycle,” *Journal of Pharmaceutical Sciences*, vol. 96, no. 12, pp. 3402–3418, 12 2007.

[46] X. Tang, S. L. Nail, and M. J. Pikal, “Evaluation of Manometric Temperature Measurement, a Process Analytical Technology Tool for Freeze-drying: Part I, Product Temperature Measurement,” *AAPS PharmSciTech*, vol. 7, no. 1, pp. E95–E103, 2006.

[47] X. C. Tang, S. L. Nail, and M. J. Pikal, “Evaluation of Manometric Temperature Measurement, a Process Analytical Technology Tool for Freeze-drying: Part II Measurement of Dry-layer Resistance,” *AAPS PharmSciTech*, vol. 7, no. 4, pp. E77–E84, 2006.

[48] X. Tang, S. L. Nail, and M. J. Pikal, “Evaluation of Manometric Temperature Measurement (MTM), a Process Analytical Technology Tool in Freeze-drying, Part III: Heat and Mass Transfer Measurement,” *AAPS PharmSciTech*, vol. 7, no. 4, pp. E105–E111, 2006.

[49] G. Reich, “Near-infrared Spectroscopy and Imaging: Basic Principles and Pharmaceutical Applications,” *Advanced Drug Delivery Reviews*, vol. 57, no. 8, pp. 1109–1143, 2005.

[50] S. Farquharson, “Pharmaceutical Applications of Raman Spectroscopy,” 2014, https://www.americanpharmaceuticalreview.com/Featured-Articles/158839-Pharmaceutical-Applications-of-Raman-Spectroscopy/, accessed on 2018-09-04.

[51] S. M. Patel and M. Pikal, “Process Analytical Technologies (PAT) in Freeze-drying of Parenteral Products,” *Pharmaceutical Development and Technology*, vol. 14, no. 6, pp. 567–587, 2009.

[52] G. Henning, W. J. Kessler, and M. Finson, “Evaluation of Tunable Diode Laser Absorption Spectroscopy for In-Process Water Vapor Mass Flux Measurements During Freeze Drying,” *Journal of Pharmaceutical Sciences*, vol. 96, no. 7, pp. 1776–1793, 2007.

[53] S. Schneid, “Process Analytical Technology (PAT) in Freeze Drying: Tunable Diode Laser Absorption Spectroscopy as an Evolving Tool for Cycle Monitoring,” *European Pharmaceutical Review*, no. 6/2009, 2009.

[54] S. Tchessalov, D. Dassu, D. Latshaw II, and S. Nulu, “An Industry Perspective on the Application of Modeling to Lyophilization Process Scale up and Transfer,” 2017.

[55] ICH, “Pharmaceutical Development Q8,” pp. 1–28, 2009.

[56] V. R. Koganti, E. Y. Shalaev, and M. R. Berry, “Investigation of Design Space for Freeze-Drying: Use of Modeling for Primary Drying Segment of a Freeze-Drying Cycle,” *AAPS PharmSciTech*, vol. 12, no. 3, pp. 854–861, 2011.

[57] O. C. Sandall, C. J. King, and C. R. Wilke, “The Relationship Between Transport Properties and Rates of Freeze-drying of Poultry Meat,” *AIChE Journal*, vol. 13, no. 3, pp. 428–438, 1967.

[58] M. Pikal, S. Shah, D. Senior, and J. Lang, “Physical Chemistry of Freeze Drying: Measurement of Sublimation Rates for Frozen Aqueous Solutions by a Micro Balance Technique.” *Pharm. Sci.*, vol. 72, no. 6, p. 635–650, 1983.

[59] K. Stan, S. Gayathri, M. Linas, and A. Alina, “LyoCalculator,” 4 2010, https://pharmahub.org/resources/lyocalculator.

[60] R. H. Bogner, “LyoModelling Calculator A New Tool to Assist in Freeze- Drying Process Design Part 2 of 2 – For Advanced Users,” https://www.spscientific.com/LyoCalc-Webinar/, accessed on 2018-09-04.

[61] R. Bogner, “LyoModelling Calculator A New Tool to Assist in Freeze- Drying Process Design Part 1 of 2 – Introduction,” https://www.spscientific.com/LyoCalc-Webinar/, accessed on 2018-09-04.

[62] SP Scientific, “LyoModelling Calculator,” https://www.spscientific.com/LyoCalc/Lyocalculator.html,accessed on 2018-09-04.

[63] A. Liapis and R. Bruttini, “A Theory for the Primary and Secondary Drying Stages of the Freeze-drying of Pharmaceutical Crystalline and Amorphous Solutes: Comparison Between Experimental Data and Theory,” *Separations Technology*, vol. 4, no. 3, pp. 144–155, 7 1994.

[64] N. Daraoui, P. Dufour, H. Hammouri, and A. Hottot, “Model Predictive Control During the Primary Drying Stage of Lyophilisation,” *Control Engineering Practice*, vol. 18, no. 5, pp. 483–494, 2010.

[65] W. J. Mascarenhasa, H. U. Akayavby, and M. J. Pikal, “A Computational Model for Finite Element Analysis of the Freeze-drying Process,” *Comput. Methods Appl. Mech. Engrg*, vol. 148, pp. 105–124, 1997.

[66] P. Sheehan and A. I. Liapis, “Modeling of the Primary and Secondary Drying Stages of the Freeze-drying of Pharmaceutical Products in Vials: Numerical Results Obtained From the Solution of a Dynamic and Spatially Multi-Dimensional Lyophilization Model for Different Operational Policies,” *Biotechnology and Bioengineering*, vol. 60, no. 6, pp. 712–728, 1998.

[67] W. Y. Kuu, L. M. Hardwick, and M. J. Akers, “Rapid Determination of Dry Layer Mass Transfer Resistance for Various Pharmaceutical Formulations During Primary Drying Using Product Temperature Profiles,” *International Journal of Pharmaceutics*, vol. 313, no. 1-2, pp. 99–113, 2006.

[68] H. Reis Sardinha, “Mechanistic Modelling of Product Degradation,” Ph.D. dissertation, Tecnico Lisboa, 2016.

[69] Process Systems Enterprise, “gPROMS ModelBuilder Documentation, Release 4.2.1 - March 2016,” https://www.psenterprise.com/sites/default/files/documentation/il/webhelp/Help.htm, accessed on 2018-09-04.